Modelling the global impact of carbon leaching from marine plastic debris on oceanic and atmospheric tracers

by

Natalia Gurgacz-Safianowicz
B.Sc. (Honours), Brock University, 2021

A thesis submitted in partial fulfillment of the
requirements for the degree of

Master of Science

in the School of Earth and Ocean Sciences

Modelling the global impact of carbon leaching from marine plastic debris on oceanic and atmospheric tracers

by

Natalia Gurgacz-Safianowicz
B.Sc. (Honours), Brock University, 2021

Supervisory Committee

Dr. Andrew. J. Weaver, Co-Supervisor (School of Earth and Ocean Sciences)

Michael Eby, Co-Supervisor (School of Earth and Ocean Sciences)

Dr. Karin Kvale, Outside Member (GNS Science)

Abstract

Since the beginning of its large-scale production in the early twentieth century, plastic remains a critical material used throughout several industries. Despite serving many benefits, plastics are resistant to degradation and instead, accumulate in the ocean and affect marine ecosystems. The leaching of toxic compounds from plastics has been widely researched, but only recently have studies begun to explore dissolved organic carbon as a leachate from marine plastic debris, as well as its effects on microbial communities. Furthermore, research has only recently begun to explore the potential effects of plastic-derived carbon leaching on the global carbon cycle and hence Earth's climate system. Here we quantify an upper bound estimate for this effect using the UVic Earth System Climate Model with the addition of global and regional carbon fluxes, based on current and projected marine plastic values. The results of these modelling integrations indicate that the addition of the plastic-derived DIC flux results in only very minor changes to the Earth's climate, emphasizing the need to focus research on plastic production and incineration-associated emissions, which are a greater threat to the climate.

Table of Contents

List of Tables

List of Figures

List of Abbreviations

Abbreviation/Term	Full Form
Alk	Alkalinity
AMOC	Atlantic Meridional Overturning Circulation
ATP	Adenosine Triphosphate
BCE	Blue Carbon Ecosystem
DIC	Dissolved Inorganic Carbon
DOC	Dissolved Organic Carbon
DOM	Dissolved Organic Matter
DON	Dissolved Organic Nitrogen
DOS	Dissolved Organic Sulphur
EPS	Expanded Polystyrene
ESCM	Earth System Climate Model
GCM	General Circulation Model
GPGP	Great Pacific Garbage Patch
MOSES	Met Office Surface Exchange Scheme
MPL	Marine Plastic Leakage
OM	Organic Matter
PA	Polyamide
PE	Polyethylene
PET	Polyethylene Terephthalate
POM	Particulate Organic Matter
PP	Polypropylene
PS	Polystyrene
PUR	Polyurethane
PVC	Polyvinyl chloride
RCP	Representative Concentration Pathway
SAT	Surface Air Temperature
SSS	Sea Surface Salinity
SST	Sea Surface Temperature

Acknowledgements

I am grateful to God for the health and strength I was granted to embark on this journey and persevere in completing this work. With great pleasure and deep gratitude, I would like to acknowledge several individuals that have supported me throughout the process of completing my master's degree and preparing this thesis. I would like to extend my deepest gratitude to my supervisors, Dr. Andrew Weaver and Michael Eby, for entrusting me as their student and guiding me along the way. Thank you for your patience, encouragement, and never failing to see my greatest potential. This has been one of my most enjoyable experiences and I am indebted to you both for that. I'm extremely grateful for the help of Dr. Karin Kvale, who provided me with insightful knowledge and suggestions, but also granted me her valuable time whenever needed. Your dedication to your work on plastic research will forever be an inspiration to me in my future work. Many thanks to the members of our lab group and my peers, Sophia Olim and Anna Nickoloff, for your assistance with problem solving and troubleshooting several lines of code, but above all, your companionship. I would like to give thanks to my parents, Krystyna and Steven, and my aunt Theresa, for the countless sacrifices they have made to further my education. Your prayers and unwavering belief in my capabilities is what has allowed me to persevere thus far. Thank you to my dear friend, Agnieszka, who brought me joy and encouragement through calls and texts, despite the distance. Last but surely not least, I would like to thank my fiancé, Adam, who tirelessly offered his love and sacrifice to help me complete this journey. With this, and all things in life, you truly reminded me to take things "one day at a time".

Chapter 1: Introduction

1.1 Plastics

1.1.1 Composition, History, and Uses

Plastics are fully synthetic materials, primarily composed of polymers, and were first developed in the form of Bakelite in 1907 (Baekeland, 1909). They are advantageous in that they can withstand a wide range of temperatures and are chemical- and light-resistant (Andrady & Neal, 2009). Additionally, their strength, durability, light weight, and low cost, are properties which drove large-scale plastic production in the early twentieth century that continues to the present day (GESAMP, 2016). Due to its unique properties, plastic was revolutionary in its time of invention and is now crucial to several industries including healthcare, transportation, construction, manufacturing, and technology. It is primarily used for packaging, building and construction, automotives, electronics, agriculture, as well as household and personal products (Plastics Europe, 2021). When sorting by resin type, polypropylene (PP), polyethylene (PE), polyvinyl chloride (PVC), polyethylene terephthalate (PET), polyurethane (PUR), polystyrene (PS) and other thermoplastics, are the most abundantly produced and found in the marine environment (Plastics Europe, 2021). Plastics are formed through addition or condensation polymerization reactions of several monomers, derived from oil or gas. Although these polymers are primarily composed of hydrogen and carbon, they rarely exist without chemicals added to improve performance and enhance their physical properties. These often include plasticizers, thermal and ultraviolet stabilizers, flame retardants, and colourings (Thompson *et al.,* 2009).

Plastics exist in various sizes and have been categorized into the following: megaplastics (>1m), macroplastics (>20mm), mesoplastics (5-20mm), microplastics (<5mm) and more specifically, nanoplastics (0.2-2mm, or anything smaller than a microplastic) (Barnes *et al.,* 2009). Marine plastic debris is typically found in the form of fragments, pellets, powders, microbeads, fibres, and foam (Morét-Ferguson *et al.,* 2010). Microplastics are widely studied in the field of marine debris as they are small and have a low density, making it easier for them to enter waterways and become ingested by organisms (Cole *et al.,* 2013; Setälä *et al.,* 2014). This allows them to act as vectors for the transfer of chemical pollutants in food chains (Teuten *et al.,* 2009). The definition and size categories of microplastics are still highly debated as authors often follow different upper and lower size limits. Frias & Nash (2019) propose a particularly descriptive definition of microplastics: “synthetic solid particle or polymeric matrix, with regular

or irregular shape and with size ranging from 1 μm to 5 mm, of either primary or secondary manufacturing origin, which are insoluble in water". Microplastics are further categorized into primary and secondary microplastic (GESAMP, 2016). Primary microplastics are originally manufactured of <5mm dimensions; these typically come from cosmetic products, industrial abrasives, insect repellents, cleaning products, and children's toys, among others. Secondary microplastics are manufactured as macroplastics and break down through photodegradation, thermal degradation, and digestive fragmentation by organisms such as microbes and krill (Dawson *et al.,* 2018; Hakkarainen & Albertsson, 2004). As plastics become increasingly fragmented, greater amounts of submicron particles are leached from these smaller plastics, since sorption in the surrounding water is more efficient (Lambert & Wagner, 2016). Though beneficial in some ways, many of these properties of plastic pose a threat to the natural environment. The following section outlines research that began to emerge in the late twentieth century with evidence of these impacts.

1.1.2 Sources of Marine Plastic Pollution

Although first thought to be the beginning of a 'brighter and cleaner' world as described by Yarsley & Couzens (1945), reports of plastic pollution began to appear in scientific literature in the early 1970s when widespread plastics were discovered in surface waters of the northwestern Atlantic Ocean, with average concentrations of 3500 particles per square kilometre, over a distance of 1300 km^2 (Carpenter *et al.,* 1972; Carpenter & Smith, 1972; Colton *et al.,* 1974; Morris, 1980; Shaw, 1977; Wong *et al.,* 1974). In 1962, plastic particles were discovered in the digestive system of sea birds, more specifically Layson Albatross (Kenyon & Kridler, 1969) and Leach's Petrels (Rothstein, 1972). Based on the data collected by Rothstein (1972), these seabirds may have ingested the plastic debris during their migration, although they typically avoid the Sargasso Sea, a region in the North Atlantic where plastics were first discovered. Given this, and the proliferation of the documented ingestion of plastics by marine organisms, researchers began to believe that the consequences of plastic pollution were more widespread temporally and geographically than initially believed.

Increased usage has driven the yearly global production of plastics from 1.5 million tonnes in 1950 (Plastics Europe, 2006) to 367 million tonnes in 2020 (Plastics Europe, 2021). Data from a study by Geyer *et al.,* (2017) showed that the cumulative global production of

plastic by 2019 would reach 9.5 billion tonnes. In addition to its increased production, plastic's lack of ability to biodegrade and its buoyancy, which may serve as benefits, are also plastic's downfall, allowing for the almost-permanent accumulation of plastics in natural environments. Plastics are resistant to rapid degradation and instead undergo slow weathering and fragmentation (Andrady, 2011). Plastics account for ~80% of all debris found in the ocean (Morales-Caselles *et al.,* 2021).

Of the 9.2 billion tonnes of global cumulative production of plastics (Mafuta *et al.*, 2021), the estimated overall volume of plastic in the ocean is 75-199 million metric tonnes (United Nations Environment Programme, 2021) with the main contributors being everyday items such as drink bottles and plastic packaging which are discarded within one year of usage (Eunomia, 2016). Population size as well as the infrastructure which countries have set in place to allow for a quality waste management system are two important factors which help determine how much marine debris is entering the ocean (Jambeck *et al*., 2015). Figure 1.1 illustrates a global map with shaded countries and their estimated mass of mismanaged waste according to the mass of plastic waste available to enter the ocean in 2010. Although most of the plastic waste that enters the ocean originates from coastal countries, a large portion is exported to countries with poor waste management and it is therefore important to note that many countries do not produce the plastic that is found on their coastlines (Law *et al*., 2020).

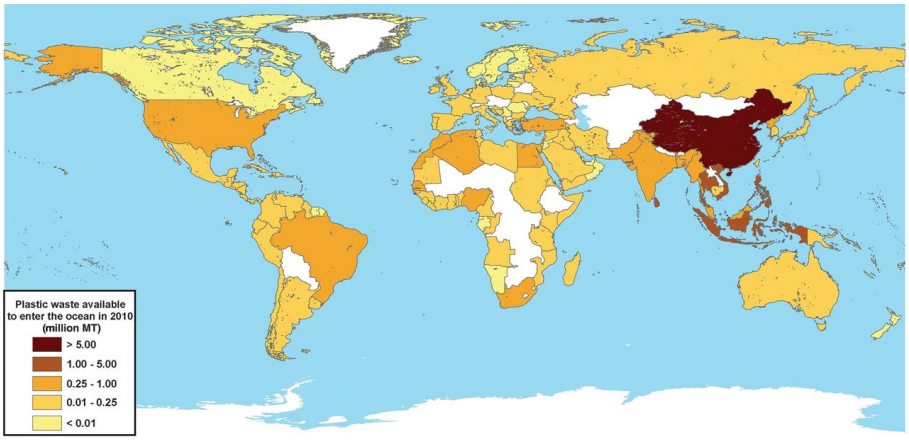

Figure 1.1. The estimated mass of mismanaged waste per country, generated in 2010 by populations living within 50 km of the coast. White areas indicate countries which were not included in the study. Reproduced from Jambeck *et al*., 2015.

Eighty percent of marine plastic input originates from land (Eunomia, 2016), from industries that include agriculture, building and construction, tourism and recreation, transportation, pharmaceuticals, and personal and healthcare products. As many coastal areas are highly urbanized and industrialized, they hold large populations of people, which ultimately leads to the greatest concentration of plastics originating from land-based coastal areas (Eunomia, 2016). Of the estimated 12.2 million metric tonnes of plastic that enter the global ocean each year, 9 million tonnes originate from land-based coastal pollution (within 50 km of the coast) (Jambeck *et al.,* 2015). Of the remaining plastic entering the ocean, 0.5 million tonnes originate from land-based inland sources, 1.75 million tonnes originate from sea-based sources (1.15 million tonnes from fishing littering and 0.6 million tonnes from shipping litter). 0.95 million metric tonnes of the total global concentration of plastics are primary microplastics, originating from marine paint, cosmetics, building and road paint, textiles, pellet spills, and vehicle tire dust (Eunomia, 2016). Modelling experiments by Onink *et al.,* (2021) revealed that the majority of land-based plastic is beached or remains floating in coastal waters, and it remains a mystery how much is entering offshore waters. As is evident by the concentrations of marine plastic listed above, land-based pollution is the number one source of marine debris, however, sea-based sources also contribute to the total volume of plastic found in the ocean. Studies have identified some major sea-based sources of microplastics which include the fisheries and aquaculture industry, offshore shipping operations, ship-based tourism, and shipwrecks (Avio *et al.,* 2015; Reddy *et al.,* 2006) which largely contribute to plastics contained in gyres (Lebreton *et al.,* 2022).

1.1.3 Pathways: From Land to Sea

The process of marine plastic entering the ocean is known as marine plastic leakage (MPL). Studies have quantified how much plastic debris is entering oceans globally; although these values differ between each paper, they range between 4.8 and 12.7 million metric tonnes per year (Ahmad & Bajahlan 2007; Jambeck *et al.,* 2015; Lebreton & Andrady, 2019; Schmidt *et al.,* 2017). It is important to differentiate the composition, shape, surface area-to-volume ratio, and density of plastic debris to better understand where it originated, its degradation rate, and predict how it will be distributed within water systems (Morét-Ferguson *et al.,* 2010; Zhu *et al.,* 2020). Research shows that low-density polymer (ie. floating) single-use plastic items, which are

difficult to recycle and easy to litter, are most likely to enter the marine environment (Addamo *et al*., 2017). As plastics become colonized by microorganisms after entering the marine environment, dense biofilms are formed on their surfaces; these so-called ecosystems have been termed the plastisphere (Zettler *et al*., 2013). Dussud & Ghiglione (2014) describe the four essential steps of the biodegradation of plastic: i) biodeterioration, which is the weakening of the plastic structure through physical and chemical deterioration by organisms adhered to the surface, ii) biofragmentation refers to the extracellular enzymes secreted by bacteria colonizing the plastic surface, ultimately reducing the molecular weight of the plastic polymers and transforming them into oligomers and monomers which are then digested by organisms, iii) assimilation, where the oligomers are integrated into the cells of microbes and can serve as a carbon source and iv) mineralization, the ultimate step of biodegradation, referring to the complete degradation of the molecules and the excretion of completely oxidized metabolites.

Plastic pollution from coastal areas makes its way offshore by wind and tidal currents (Chassignet *et al*., 2021; Dobler *et al*., 2019; Jambeck *et al*., 2015). Land-based plastic debris is entering marine environments through stormwater runoff, wind dispersal, inadequate waste and disposal management such as dumps or uncontrolled landfills, and littering (Jambeck *et al*., 2015; Lebreton *et al*., 2017). The Pew Charitable Trusts (2020) identified four main routes through which land-based debris flows into the ocean. These include a) uncollected waste on land that makes its way into water b) uncollected waste which is directly dumped into water c) collected waste that is deposited into dumpsites that move via land and air into water d) collected waste that is dumped directly into water by collection trucks. Once plastic debris enters the ocean, it is transported both vertically and horizontally throughout the ocean. Horizontal transport of plastics is influenced by a combination of surface residual currents and wind-driven currents (Isobe *et al*., 2014; Liubartseva *et al*., Iwasaki *et al*., 2017). The horizontal distribution of plastic is variable as it is also impacted by coastline geography and the location of the point of entry into the marine environment (Barnes *et al*., 2009). Analysis of the vertical transport of plastics throughout the water column indicates that most items are suspended within upper layers through advection transport and turbulent mixing (Kukulka *et al*., 2012), and concentrations drop exponentially as depth increases (Reisser *et al*., 2015). The vertical distribution of plastics in the ocean is dependent on the particle density, surface area of the polymer, and the size and shape of the particle (Kowalski *et al*., 2016).

When investigating the occurrence and distribution of microplastics off the United States' southeastern coast, results indicate that given the dominant shape and type of polymers found, most plastics originate from wastewater discharge from urban areas rather than through the breakdown of macroplastics (Yu *et al.,* 2018). Several studies have found that rivers act as a major transport pathway for inland plastic debris with small urban rivers being the most polluted; 67% of the total global plastic debris is brought into the ocean via the world's top twenty polluted rivers (Lebreton *et al.,* 2017; Meijer *et al.,* 2021; Schmidt *et al.,* 2017; United Nations Environment Programme, 2021). Seven of the world's top ten plastic-polluted rivers are found in the Philippines, with two in India and one in Malaysia (Meijer *et al.,* 2021). Additionally, Meijer *et al.,* (2021) describe the characteristics of the largest emitting rivers, those being: near poor waste management sites, near urban cities with paved roads where water and plastics can drain into river basins, in regions with high precipitation rates and high flow rates from rivers to the ocean, and finally, near the coast. As plastics leave their land- and sea-based sources, they follow various pathways based on their differences in composition, eventually congregating in specific areas of the ocean.

1.1.4 Accumulation Zones

As plastic particles become increasingly degraded, weathered, and biofouled over time, their size, shape, and density change, ultimately resulting in different transport pathways and fates. Plastics collected in mid-ocean gyres, for example, are being identified as having a small surface area-to-volume ratio indicating that only certain types of debris can move with winds and ocean currents to accumulate in these regions (Lebreton *et al.,* 2018). There are varying results regarding the dominant polymer types and shapes found in the marine environment. The most frequently found polymer types include PET, PE and PP; fibres, fragments, and filaments are the most frequently found shapes (Yu *et al.,* 2018; Wang *et al.,* 2020). PE and PP tend to float in the water column as their densities are lower than that of seawater, whereas PVC, PS, PET, and PA sink, as their densities are greater than that of seawater (Guo & Wang, 2019). Additionally, resin types such as PE and PP, which normally float, have been found in marine sediments as they become biofouled and sink due to the increase in density (Morét-Ferguson *et al.,* 2010).

As of 2014, over 5 trillion plastic pieces, weighing 250 000 tonnes were afloat at sea (Eriksen *et al.,* 2014). It is estimated that the ocean contains 150 million tonnes of plastic, based

on global production since 1950 (McKinsey, 2015). As the quantities of buoyant plastic waste are much lower than the estimated quantity of mismanaged waste entering from land, there is a large fraction of plastic that is unaccounted for (Cózar *et al.,* 2014; Eriksen *et al.,* 2014; Isobe & Iwasaki, 2022). Lebreton *et al.,* (2019) created a global model of ocean plastics from 1950 – 2015, which indicates that most plastic waste has been accumulating along shorelines. Further studies, including Chassignet *et al.,* (2021), show that of the marine plastic waste that was released from 2010 to 2019, 75.4% remained on coasts whereas 25.5% entered the ocean. The settling of these plastics in deep-sea regions of the ocean is strongly controlled by thermohaline currents; deep-sea biodiversity hotspots are likely microplastic hotspots as well (Kane *et al.,* 2020). There are, however, regional differences in the concentration of microplastics found in both surface waters and sediment, with the lowest concentrations being in remote areas; studies have shown that plastics are now accumulating in the top sediment layer of the deep sea (Fischer *et al.,* 2015; Van Cauwenberghe *et al.,* 2013). They are accumulating at depths ranging from 1100 to 5000 meters and are being ingested by deep-sea organisms (Jamieson *et al.,* 2019; Taylor *et al.,* 2016). Plastics are embedded below the surface of shorelines up to depths of 2 meters and microplastic fragments are found in marine sediments (Loughlin *et al.,* 2021; Turra *et al.,* 2014). Microplastics are also appearing in polar waters (Obbard, 2018; Jones-Williams *et al.,* 2021), Arctic Sea ice (Obbard *et al.,* 2014) and Antarctic ecosystems (Caruso *et al.,* 2022).

First discovered in the 1970s (Venrick *et al.*, 1973; *Wong et al.*, 1974) the largest oceanic accumulation of plastics is known as the Great Pacific Garbage Patch (GPGP) in the Northern Pacific subtropical gyre, holding an estimated 79 thousand tonnes of plastic floating in an area of 1.6 million km^2 (Lebreton *et al.,* 2018). Similar to the GPGP, marine plastics accumulate in regions of convergence of ocean currents (Law *et al.,* 2014; Martinez *et al.,* 2009). Garbage patches have also been observed in the western North Pacific Ocean near the Kuroshio Extension (Yamashita & Tanimura, 2007) as well as in the western North Atlantic subtropical gyre (Law *et al.,* 2010). With the continuous rise in plastic production and minimal efforts being made for plastic pollution mitigation, it is no surprise that marine plastic pollution rates are expected to increase. Annual rates of aquatic plastic pollution are expected to nearly triple, to 29 million metric tonnes by 2040, according to the 'business-as-usual' scenario modelled by Lau *et al.,* 2020 (Figure 1.2).

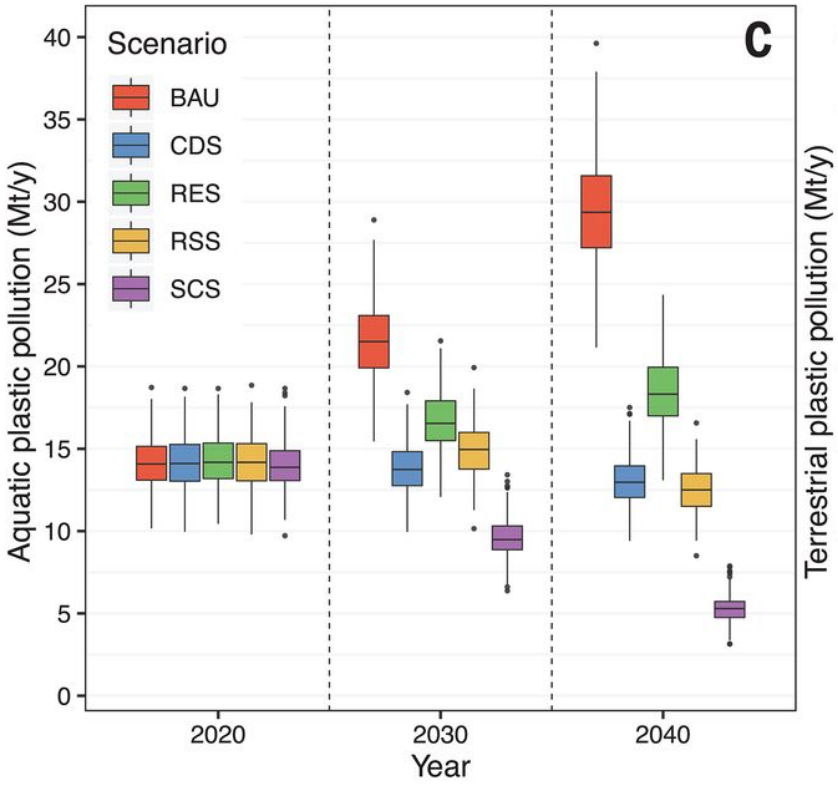

Figure 1.2. Annual rates of plastic pollution estimated from 300 Monte Carlo simulations. Boxplot of plastic pollution entering aquatic ecosystems for the years 2020, 2030, and 2040. Scenarios include: Business as Usual (BAU), Collect and Dispose scenario (CDS), Recycling scenario (RES), Reduce and Substitute scenario (RSS), and System Change scenario (SCS). Further explanation and definition of scenarios can be found in Lau et al., (2020).

1.1.5 Dangers of plastics in the marine environment

Interest in plastic research is rising due to the concern of plastics entering biotic realms and becoming hazardous to organisms. Plastics of various sizes have been found in the intestinal tracts of marine species including planktivores, detritivores, filter- and suspension-feeders, echinoderms, molluscs, seabirds, and mammals, amongst others (Boerger *et al.,* 2010; Botterell *et al.,* 2020; Grant *et al.,* 2021; Naji *et al.,* 2018; Wright *et al.,* 2013). Some plastics appear similar to the food consumed by organisms, leading them to ingest or become entangled in plastic debris. Eventually, these plastics accumulate in humans as they reach higher trophic levels within the food web (Thushari & Senevirathna, 2020). A paper published by Leslie *et al.,* (2022), where polymers from plastic were detected and quantified in human blood, alarmed many. In addition to the ability of plastics to adsorb toxic compounds and heavy metals in the marine environment (Prinz & Korez, 2020; Verla *et al.,* 2019), they can also transport invasive

species (Garcia-Gómez *et al*., 2021). Studies discuss how these plastics and the toxic compounds they come with, have resulted in a range of effects on organisms including physical abrasions and blockages, reduced reproductive fitness, diminished enzyme production, and nutrient dilution, even showing effects on the cellular level (Biagi *et al*., 2021; Prinz & Korez, 2020).

In the field of marine plastic pollution, research focuses on the leaching of compounds such as metals, phenols and phthalates and other contaminants (Montoto-Martínez *et al*., 2021; Paluselli *et al*., 2018), however, little research has been done on the contribution of non-pollutant type compounds from plastics after they enter the marine environment. Most studies focus on the distribution and size classes of plastics, and so, more research must be done on the effects of their biodegradation on biota (Romera-Castillo *et al*., 2018). Compounds like carbon, for example, are being leached from plastics in the ocean and are resulting in disruptions to microbial organisms and carbon cycling (Cheng *et al*., 2021; Romera-Castillo *et al*., 2018). As plastic production and its presence in the natural environment continue to grow, it is important to continue studying the global and long-term effects that plastics may have on all forms of life on Earth.

1.2 Carbon

1.2.1 The Carbon Cycle

Carbon is the building block of life on Earth; it is unique in that it can form single, double, and triple covalent bonds with other atoms, allowing it to become the backbone of important biomolecules including nucleic acids, adenosine triphosphate (ATP), carbohydrates, lipids and fats, proteins, lignans, chitin etc. These stable bonds allow for the chemical versatility necessary for the growth and replication of cells, and ultimately, life (Pace, 2001). In addition to being one of the most abundant higher elements, carbon is also able to form bonds with other carbon atoms, allowing for large and complex molecules to be built (Pace, 2001). The process of carbon cycling throughout near-surface reservoirs including sediments, oceanic waters, terrestrial and aquatic biomass, soils, and the atmosphere is known as the exogenic carbon cycle (Lerman, 2009); it cycles through the dynamic Earth from one realm to another. Major carbon reservoirs include the atmosphere, ocean, and terrestrial systems which include forests and soil (Figure 1.3). The carbon cycle involves CO_2 being dissolved in rain, land, and ocean surface waters and is converted from inorganic to organic carbon by photosynthesizing biota. Organisms also

convert carbon from the organic to the inorganic form through the process of cellular respiration which enters soil through decomposing organic matter. Carbon is exchanged in the form of CO_2 between the atmosphere and vegetation, soil, and surface waters; it is released into the atmosphere through volcanic eruptions and fossil fuel combustion. The carbon cycle further involves the dissolution of CO_2 into bodies of water through turbulent mixing which occurs near the air-sea boundary where a small fraction is converted from the gaseous to the aqueous form and the majority is converted into HCO_3^- and CO_3^{2-}. It also involves the incorporation of carbon from the ocean into the atmosphere through outgassing, the entrance of organic carbon into the ocean and its rapid breakdown by microbes into dissolved inorganic carbon (DIC) with a small fraction remaining as dissolved organic carbon (DOC), and the deep sea through decomposing marine biota that eventually becomes incorporated in sediment (Figure 1.3). In the ocean, DIC is absorbed by autotrophic marine biota, and converted into DOC, and all biotas produce DIC through cellular respiration and decomposition (Figure 1.3; NOAA, 2019).

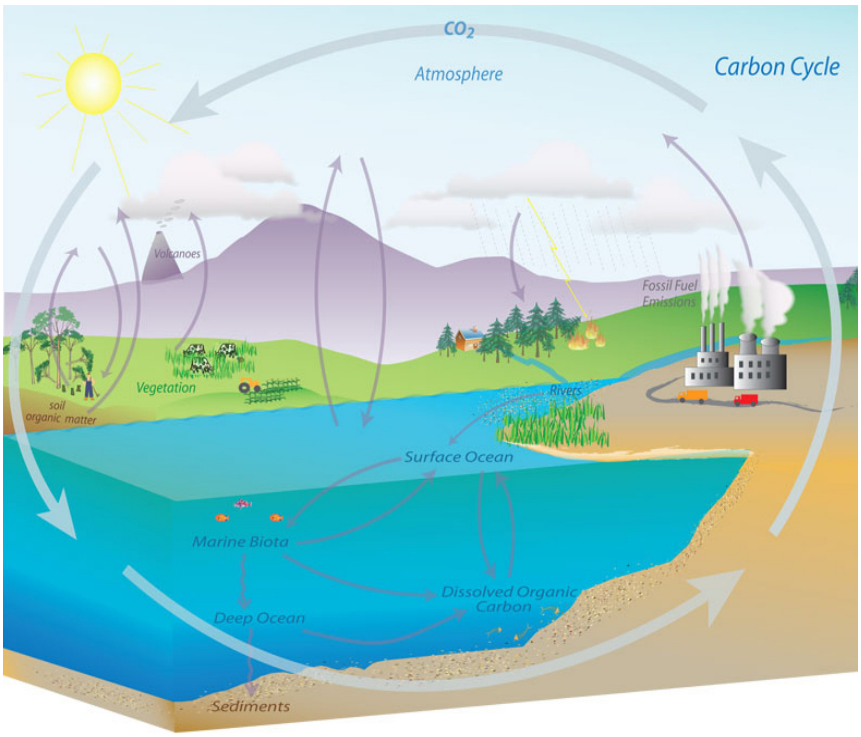

Figure 1.3. The Carbon Cycle. The above figure displays the cycling of carbon through Earth's atmosphere, ocean, vegetation, and sediments. Reproduced from the National Oceanic and Atmospheric Administration (NOAA, 2019).

Anthropogenic carbon perturbations are resulting in an unbalanced carbon cycle. Anthropogenic emissions, resulting from activities including the combustion of fossil fuels,

cement production, deforestation, agricultural practices, and land-use change, are increasing 0.1 GtC/y (Friedlingstein *et al.,* 2022). Currently, the ocean is acting as a carbon sink as it takes in more carbon than it releases, however, through the process of air-sea exchange, whereby atmospheric CO_2 moves across the air-sea boundary and enters surface waters, the concentrations of carbon in the ocean will impact those in the atmosphere, and vice versa (Lerman, 2009). The exchange of CO_2 between this boundary is dependent on the following: the mass of CO_2 in the atmosphere, the temperature, salinity, and chemical composition of the water, biological production and respiration rates of organic matter (OM), and the precipitation and dissolution rates of $CaCO_3$ (Lerman, 2009).

1.2.2 Carbon in the Marine Environment

Oceanic OM exists as particulate organic matter (POM) (>0.45 μm in size, is mostly composed of detritus, and when it enters aquatic environments it can be suspended in the water column or sink to the sediments. OM also contains dissolved organic matter (DOM) (< 0.45 μm in size, which is mostly lifeless and remains in the water column. DOM is primarily composed of molecules including carbon (DOC); it contains a comparable amount of carbon (662 Pg C) (Hansell *et al.,* 2009) to the atmosphere. DOC is used for the fueling of marine food webs and makes up a large component of the carbon cycle (Hansell *et al.,* 2009). The majority of DOC is labile, meaning that it can be rapidly broken down (within hours or days) by microbes and bacteria for biomass production and respiration, ultimately producing DIC. The small fraction of DOC that is resistant to microbial degradation and breaks down on time scales of thousands to tens of thousands of years, is known as recalcitrant DOC. Through the process of respiration or decomposition, DOC is broken down into DIC, which is composed of HCO_3^-, CO_2, and CO_3^{2-}, with HCO_3^- making up the largest fraction of DIC. These oxidized forms of carbon are the most abundant form of carbon at the Earth's surface (Lerman, 2009). DIC is mainly influenced by the biological pump (a carbon sub-cycle) where through photosynthesis, this inorganic carbon is fixed into organic carbon and eventually sequestered into the deep ocean. Another sub-cycle of the carbon cycle, the carbonate or carbonate counter pump, is the process whereby oceanic biota combine Ca^{2+} and CO_3^{2-} to form calcium carbonate ($CaCO_3$). Finally, the solubility pump, is the process of dissolution of atmospheric CO_2 in seawater through the air-sea interface, in order to

maintain chemical equilibrium. This CO_2 dissolves and forms DIC in surface waters, which eventually sinks and enters the deep ocean.

Marine DOC originates from autochthonous and allochthonous sources (Lønborg *et al.,* 2020). Autochthonous sources, derived from within the ocean, include primary producers by phytoplankton, macroalgae and seagrass (Anderson & Hillwalker, 2008). Allochthonous sources, originating from outside the ocean, include groundwater, melting glaciers and sea ice, rivers, as well as rain and dust from the atmosphere (Willey *et al.,* 2000). Given that plastics, originating from outside the ocean, add to the marine DOC pool, one could consider plastic debris an allochthonous source of DOC. Although carbon emissions released during the production of plastic are widely studied, carbon emissions released in the marine environment are only beginning to be explored.

1.2.3 Plastic-Derived Carbon Leaching

"Plastic is a vector of carbon"; with plastic being inherently carbon, and travelling throughout the global water system, plastic transfers carbon from one reservoir to the next (Zhu *et al.,* 2021). Studies done by Romera-Castillo *et al.,* (2018) and Zhu *et al.,* (2020) will be heavily discussed throughout this thesis as these are two primary studies which specifically looked at DOC leaching by microplastics in marine environments. The process of leaching occurs when solutes, for example, chemicals and compounds, become detached from a solid material when it encounters a solvent. Romera-Castillo *et al.,* (2018) hypothesized that the millions of metric tonnes of plastic that are in the ocean are contributing to the DOC pool through leaching. It was found that PP and PE leach DOC into ambient water under irradiant and dark conditions in a study by Romera-Castillo *et al.,* (2018). Plastics leached DOC only under irradiated conditions in a study by Zhu *et al.,* (2020), with expanded polystyrene (EPS) leaching the greatest amount of DOC. Zhu *et al.,* (2020) similarly looked at DOC released from buoyant microplastics and found that EPS degrades faster than both PP and PE due to the presence of aromatic, sunlight-absorbing structures which have been shown to rapidly degrade in the surface ocean (Gewert *et al.,* 2015). The results from Romera-Castillo *et al.,* (2018) show the highest leaching concentrations occurring when the plastic first contacts seawater followed by an exponential decrease. On the contrary, Zhu *et al.,* (2020) showed an increase in DOC leaching by some plastics and a steady leaching rate by others as time increased. It was stated that this

difference may have been due to differences in experimental design (Zhu *et al*., 2020). One may argue that both methods were accurate as Romera-Castillo *et al*., (2018) observed the initial entrance of plastics into the ocean while Zhu *et al*., (2020) pre-rinsed the plastic, simulating a sustained release of DOC. Based on the estimated inflow rate of plastics each year by Jambeck *et al*., (2015), and the range of leached DOC in the study by Romera-Castillo *et al*., (2018), it was estimated that between 260 – 23, 600 metric tonnes of DOC could be leached from plastics into surface waters each year. In areas with very high surface water concentrations of plastics, particularly in subtropical gyres, up to 10 ± 0.3% of the DOC in the surface microlayer of those gyres, could originate from marine plastic debris (Romera-Castillo *et al*., 2018).

Since this research was published, there has been greater concern around the topic of plastic-derived carbon leaching. Although little is yet known about the scale of this leaching, researchers have discussed the importance of considering plastic to be part of the global carbon cycle and have encouraged greater research on the matter. Adyel & Macreadie (2022) present a modelled estimate of the mass of plastic-derived carbon from coastal plastic pollution assuming an 83% conversion from plastic to carbon in gyres (Zhu *et al*., 2020; Figure 1.4). Adyel & Macreadie (2022) further describe the potential concerns with having plastic-derived carbon leaching near coastal areas and the effects of imbalances in the oceanic carbon pool.

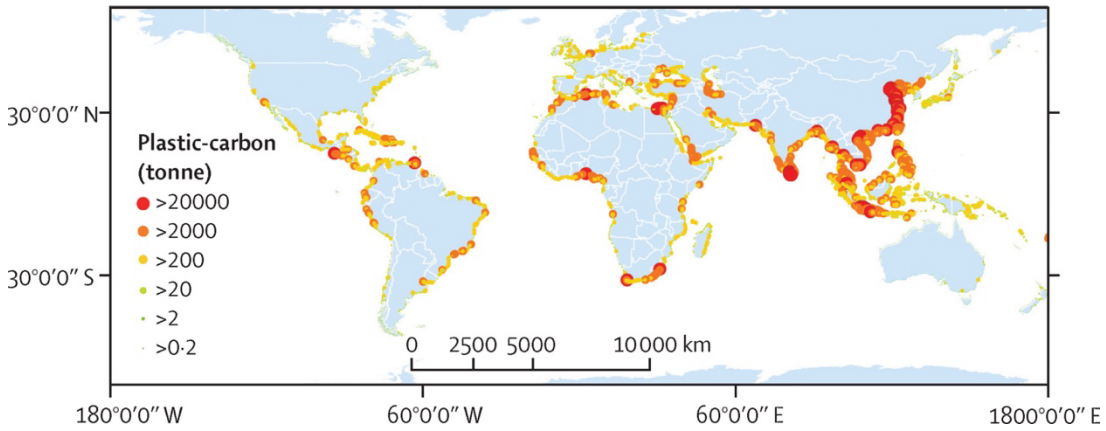

Figure 1.4. The above figure displays the modelled mass of plastic-derived carbon (tonnes) based on plastic waste discharged from land into coastal areas (Lebreton & Andrady, 2019), and the plastic to carbon conversion (Zhu *et al*., 2020). Reproduced from Adyel & Macreadie, 2022.

1.2.4 Effects of Marine Carbon Imbalances

As stated by Lønborg *et al*., (2020), the ocean DOC pool is very large and small changes in inputs and removal could result in substantial net changes in the ocean carbon cycle and climate, as the interconnectedness of the carbon cycle leads to many downstream effects on ocean processes. Romera-Castillo *et al*., (2018) and Zhu *et al*., (2020) also discussed the effects of plastic-derived carbon leaching on microbial communities as these organisms take up DOC. Changes in the timing of microbial growth and abundance were observed, in addition to bio-inhibitory activity after the exposure to plastic-derived DOC, ultimately resulting in changes in community structure and composition (Romera-Castillo *et al*., 2018). There is a growing concern about the effects of plastic-derived carbon leaching on blue carbon ecosystems (BCEs), which are comprised of tidal marshes, mangrove forests, and seagrass meadows, and act as major sinks of carbon dioxide (Adyel & Macreadie, 2022). Long-term increases in the ocean's surface water DOC pool can result in a variety of environmental and socio-economic changes including impacts on freshwater biota, drinking water quality, coastal marine ecosystems, and carbon imbalances (Evans *et al*., 2005). In addition, although the ocean's primary producers can process carbon, excess CO_2 can lower the ocean's pH and result in ocean acidification. This can lead to the dissolution of $CaCO_3$, affecting organisms including oysters, corals, abalone, scallops, mussels and other shelled molluscs, that depend on this compound for the formation of their shells (Haigh *et al*., 2015).

The above concerns mainly focus on the biological effects of plastic-derived carbon leaching, specifically on microbial communities, as the carbon being leached from marine plastic pollution is in the form of DOC. To consider the effects on the global climate, it is important to consider the change in concentrations of oceanic and atmospheric inorganic carbon as a result of plastic-derived carbon leaching. The next chapter of this thesis describes the methodology and purpose behind the present study and how it will attempt to quantitatively analyze the effects of marine plastic-derived carbon leaching on the global climate. The goal of this thesis will be to fill gaps in knowledge proposed by researchers in marine plastic pollution and global climate fields.

1.3 Present Study

As discussed here, recent literature has focused on the release of carbon from plastic debris in the marine environment, and whether this amount is substantial enough to result in changes in Earth's global climate system. Research suggests that this increase in oceanic carbon may disrupt ecological communities, carbon sequestering ecosystems, as well as our general climate system, through increased atmospheric CO_2 levels. These statements have been made without concrete evidence of plastic carbon significantly contributing to anthropogenic CO_2. To further explore the severity of this problem, a series of climate modelling experiments were performed which involved the input of a DIC flux, derived from upper-bound current and projected marine plastic values, into various regions of the global ocean, over time. In doing so, we can quantitively measure the impact that this upper-bound carbon flux, which represents the maximum addition of plastic-derived DIC, and the effects this may have on oceanic and atmospheric tracers.

The research presented in this thesis involves the use of the intermediate complexity, University of Victoria, Earth System Climate Model (UVic ESCM) to quantify the climatic effects of an upper-bound of plastic carbon leaching into the surface ocean, on a global scale. With the use of the model, current and projected plastic-derived DIC fluxes were added to various regions of the ocean over 100 or 500 years, and the effects on oceanic and atmospheric tracers were observed. The next chapter of my thesis, Chapter 2, describes the methodology of the performed model integrations as well as background details on the model itself. Chapter 3 displays the results of the model runs as well as descriptions of the main results. Chapter 4 includes a description of the meaning and relevance of the results. Finally, the last section of my thesis provides a summary of my findings and provides suggestions for future work relating to emissions from plastic production and incineration.

Chapter 2: Methodology

2.1 The UVic ESCM Background

The model results presented in this thesis are from climate modelling experiments using version 2.9 of the intermediate-complexity University of Victoria Earth System Climate Model (UVic ESCM; Weaver *et al.,* 2001). This model includes a two-dimensional atmospheric energy-moisture balance model (Fanning & Weaver, 1996), a three-dimensional ocean general circulation model (Pacanowski, 1995), a dynamic-thermodynamic sea ice model (Bitz *et al.,* 2001) with elastic visco-plastic rheology (Hunke and Dukowicz, 1997), and a land surface and dynamic-vegetation model based on the Hadley Centre Met Office Surface Exchange Scheme (MOSES) coupled to the Top-down Representation of Interactive Foliage and Flora with five plant functional types (Cox, 2001; Meissner *et al.,* 2003). All components of this model exhibit a spherical grid resolution of 3.6° (in the zonal direction) and 1.8° (in the meridional direction) and the ocean component includes 19 vertical levels, with thickness varying from 50m near the surface to 500m in the deep ocean. Radiative forcings, which are associated with changes in atmospheric CO_2 concentrations, are included as changes in outgoing planetary longwave radiation. Surface wind stress and atmospheric winds are specified from 40-year climatologic reanalysis data from the National Centers for Environmental Prediction (NCEP) project (Kalnay *et al.,* 1996). An oxic-only ocean sediment model has been added to the UVic ESCM, whereby simulations of $CaCO_3$ preservation in deep-sea sediments are represented (Archer, 1996), in addition to a nutrient-phytoplankton-zooplankton-detritus marine ecosystem model component (Schmittner *et al.,* 2008).

This model was spun up with forcing for the year 850 over 10 000 years with only seasonal variation in solar radiation and surface winds, and constant CO_2 concentrations. The year 2000 initial condition for all experiments shown in Table 2.1 was obtained by starting from the 10 000-year equilibrium spin-up and applying transient historical forcing until the year 2000 (see Eby *et al.,* 2009 for details). Beyond the year 2000, a single 500-year transient forcing simulation was performed with Representative Concentration Pathway (RCP) 8.5 specified forcings, CO_2 concentrations, and the equivalent CO_2 emissions were diagnosed by the model. Beyond the year 2300, year-2300 specified forcing only varied seasonally. The diagnosed emissions from this simulation were then used as CO_2 emissions from fossil fuels for all other simulations beyond the year 2000. This allowed the model to react to changes in CO_2

concentrations rather than be constrained by specified concentrations. (IPCC, 2008; Eby *et al*., 2009).

The UVic ESCM can simulate the air-sea flux of CO_2, the distribution of DIC and alkalinity, the percent of $CaCO_3$ in sediments, global carbon budgets, and observation-based surface-air temperature and CO_2, over time. The inorganic carbon component of the model is based on the ocean carbon-cycle model intercomparison project (OCMIP; Orr *et al*., 1999). The comprehensive carbon cycle component is further described by Eby *et al*., (2009). The use of this intermediate-complexity model allows one to perform numerical experiments that are more computationally efficient compared to coupled general circulation models (GCMs). Further details of the UVic ESCM are explained in Weaver *et al*., (2001).

2.2 Methodology of Current Study Modelling Experiments

To observe the upper-bound effects of plastic-derived carbon leaching using the UVic ESCM, a mask was created and applied to the model in order to only add post-leaching carbon fluxes to specific areas of the world's oceans. This method was efficient in that it allowed for the sole focus to be on the carbon-leaching component of marine plastic pollution without the need to incorporate the leaching process from plastic to seawater into the model. Most model integrations were run for 100 years from the year 2000 to 2100 (see Table 1). Output from these integrations was averaged and recorded every 10 years. Additional output was produced at the end of the 100-year model integrations. Longer model integrations were run for 500 years from the year 2000 to 2500 (see Table 1). Output from these model integrations was averaged and recorded every 100 years. Additional output was produced at the end of the 500-year model integrations.

To observe the largest potential consequences of carbon leaching on the Earth's systems, it was assumed that the maximum potential amount of plastic would enter the ocean and the maximum potential amount of carbon would be leached from the plastic debris into the marine environment. Therefore, the upper bounds of both current and projected global marine plastic flux values found in the literature were used in all model integrations. Plastic-derived DIC flux values were calculated based on the current yearly global input of plastic (4.8-12.7 million metric tonnes per year; Jambeck *et al.,* 2015) and the upper bound yearly rate (12.7 million metric

tonnes) was used for model runs CUR-G and CUR-NA (Table 1). For the context of this study, DIC derived from marine plastic will be referred to as plastic-derived DIC.

Table 2.1. Configuration of model integrations used in this study.

Model Run Name/Abbreviation	Model run length (years)	Value of plastic-derived DIC flux ($\mu mol\ cm^{-2}\ sec^{-1}$)	Location of plastic-derived DIC flux addition
Control	100, 500	-	-
CUR-G	100	9.36×10^{-9}	Global Ocean
CUR-NA	100	2.97×10^{-7}	North Atlantic Ocean
PROJ-G	100	2.15×10^{-8}	Global Ocean
PROJ-NA	100	6.82×10^{-7}	North Atlantic Ocean
PROJ-NP	100	7.63×10^{-7}	North Pacific Ocean
PROJ-IND	100	5.62×10^{-7}	Indian Ocean
PROJ-SA	100	7.62×10^{-7}	South Atlantic Ocean
PROJ-SP	100	5.18×10^{-7}	South Pacific Ocean
PROJ-NA-500	500	6.82×10^{-7}	North Atlantic Ocean
PROJ-SA-500	500	7.62×10^{-7}	South Atlantic Ocean
PROJ-COA	100	2.04×10^{-7}	Global coast
PROJ-COA-500	500	2.04×10^{-7}	Global coast

Column 1 displays the labels of each model run including the control and 12 modelling experiments. Column 2 displays the run length (in years) of each modelling run. Column 3 displays the DIC flux value ($\mu mol\ cm^{-2}\ sec^{-1}$) based on the current or projected marine plastic values and the surface area of each location of the input. Column 4 displays the locations into which the plastic-derived DIC flux value was added.

Due to the limitations of the UVic ESCM, fluxes of DIC, rather than DOC, were added into the specified locations of the ocean, as DIC is the only form of dissolved carbon that is prognostically retained within the model. For this study, all forms of carbon released by plastic debris in the ocean were categorized as DIC. This is an acceptable substitute, as natural labile DOC breaks down rapidly and contributes to the ocean DIC pool rather than the organic carbon pool (Hansell *et al*., 2013). By assuming the complete conversion from DOC to DIC, we can estimate the upper bound effects of plastic-derived carbon leaching on the global climate system. Zhu *et al*., (2020) determined that 83% of carbon was being leached from plastic into seawater in

gyres, however, all the model runs in this study assumed a 100% conversion from plastic to DIC to further provide a maximum upper bound result.

Using the 100% conversion, the molar mass of carbon (12.0 g/mol), and the total surface area of the global ocean from the model (3.57 x 10^{18} cm^2), plastic fluxes were converted to UVic ESCM DIC fluxes units of μmol cm^{-2} sec^{-1} as presented in equations 2.1a, 2.1b and 2.1c. These equations demonstrate how the plastic-derived DIC flux was calculated for the input into the global ocean, whereas other fluxes were calculated based on their respective oceanic surface areas (Table 1).

$$\frac{12.7 \text{ x } 10^6 \; tonnes \; of \; plastic}{yr} \cdot \frac{1 \text{ x } 10^6 \; g}{tonne} = \frac{1.27 \text{ x } 10^{13} \; g}{yr} \qquad 2.1a$$

$$\frac{1.27 \text{ x } 10^{13} \; g}{yr} \cdot \frac{1 \; mol}{12.0 \; g \; of \; C} \cdot \frac{1 \text{ x } 10^6 \; \mu mol}{1 \; mol} = \frac{1.06 \text{ x } 10^{18} \; \mu mol}{yr} \qquad 2.1b$$

$$\frac{1.06 \text{ x } 10^{18} \; \mu mol}{yr} \cdot \frac{1}{3.57 \text{ x } 10^{18} \; cm^2} \cdot \frac{1 \; yr}{365 \; d} \cdot \frac{1 \; d}{24 \; h} \cdot \frac{1 \; h}{60 \; min} \cdot \frac{1 \; min}{60 \; s} = 9.36 \text{ x } 10^{-9} \frac{\mu mol}{cm^2 \cdot s} \qquad 2.1c$$

DIC flux values as indicated in Table 1 are different for each location of input into the subtropical gyres as these values were calculated based on their specified surface areas. They are as follows: 1.12 x 10^{17} cm^2 (North Atlantic), 1.00 x 10^{17} cm^2 (North Pacific), 1.36 x 10^{17} cm^2 (Indian Ocean), 1.01 x 10^{17} cm^2 (South Atlantic), 1.48 x 10^{17} cm^2 (South Pacific).

Projected plastic-derived DIC values were calculated based on reported results by Lau *et al.,* (2020) which state that given the current trajectory of plastic production, the amount of plastic going into the ocean will almost triple by 2040 to a rate of 29 million metric tonnes per year, equivalent to 50 kg of plastic per metre of coastline worldwide. The plastic-derived DIC flux was calculated similarly to Equations 2.1a, 2.1b and 2.1c, except the initial global plastic flux was 29 million metric tonnes per year rather than 12.7 million.

The coastal flux was also calculated in a similar way in equations 2.2a, 2.2b and 2.2c, however, this calculation had to account for the initial unit difference of kg m^{-1} $year^{-1}$ (50 kg of plastic per metre of coastline (Lau *et al.,* 2020); Equation 2.2a). This calculation also had to incorporate the multiplication of the flux by the total length of all coastlines in the model (2.93 x 10^{10} cm) divided by the total surface area of all coastal grid boxes (3.75 x 10^{17} cm^2) in equation 2.2c. Since the model cannot account for small convolutions in the Earth's coast or many unresolved islands, the calculated flux being distributed along the coast had to be multiplied by a

factor of 1.98 (in equation 2.2c) to accommodate the difference in coast length in the model versus the Earth's actual coastal length. This factor was determined by calculating the difference between the total coastal flux (14.65 million tonnes) which incorporated the model's coast, versus the flux provided by Lau *et al*., (2020): 29 million tonnes.

$$\frac{50\ kg}{m \cdot \text{yr}} \cdot \frac{m}{100\ cm} \cdot \frac{1000 g}{kg} \cdot \frac{mol}{12.0\ g} \cdot \frac{1 \text{ x } 10^6\ \mu mol}{1\ mol} = \frac{4.16 \text{ x } 10^7\ \mu mol}{cm \cdot \text{yr}} \quad 2.2a$$

$$\frac{4.16 \text{ x } 10^7\ \mu mol}{cm \cdot \text{yr}} \cdot \frac{1\ yr}{365\ d} \cdot \frac{1\ d}{24\ h} \cdot \frac{1\ h}{60\ min} \cdot \frac{1\ min}{60\ s} = \frac{1.32\ \mu mol}{cm \cdot s} \quad 2.2b$$

$$\frac{1.32\ \mu mol}{cm \cdot s} \cdot 2.93 \text{ x } 10^{10}\ cm \cdot \frac{1}{3.75 \text{ x } 10^{17} cm^2}\ 1.98 = \frac{2.04 \text{ x } 10^{-7}\ \mu mol}{cm^2\ s} \quad 2.2c$$

Thirteen modelling integrations were performed, including both current and projected plastic-derived DIC values, which were distributed globally (model runs CUR-G, PROJ-G), distributed evenly into all global coastlines (model runs PROJ-COA, PROJ-COA-500), as well as added into specified locations in the world's oceans (model runs CUR-NA, PROJ-NA, PROJ-NP, PROJ-IND, PROJ-SA, PROJ-SP, PROJ-NA-500, PROJ-SA-500), over a 100- or 500- year period (Table 1). In addition, a control run was performed which did not include the addition of the plastic-derived DIC flux. For DIC fluxes which were added into specific regions of the world's oceans, the total flux value that would typically be distributed amongst all grid boxes of the global ocean was instead distributed within the specified area of the ocean, ultimately increasing the DIC flux value applied over that area. The purpose of these model runs was to measure the potential impacts that lower versus higher DIC flux values may have on Earth's climate system and the effect of applying the plastic-DIC flux in high concentrations into various regions of the ocean.

CUR-G included a current plastic-derived DIC flux which was distributed evenly across the global ocean over a 100-year period. CUR-NA also included a current plastic-derived DIC flux, however, the flux was instead added into a specified area in the ocean, over a 100-year period, with the prediction of a higher concentration of DIC having a greater impact on Earth's processes. The North Atlantic Ocean was chosen as the specified area of input, as this is an area that may impact the Atlantic meridional overturning circulation. This model run specifically included the addition of DIC into the North Atlantic subtropical gyre region, as evidence has shown that perturbations, such as this additional DIC flux, could interact with deep water

formation in the North Atlantic Ocean, which will later be discussed in the Discussion section of this thesis. PROJ-G included a projected plastic-derived DIC flux which was distributed evenly across the global ocean for 100 years. Model runs PROJ-NA, PROJ-NP, PROJ-IND, PROJ-SA, and PROJ-SP included a projected plastic-derived DIC flux which was added into specified areas of the global ocean over a 100-year period; the total DIC flux was added into either the North Atlantic, North Pacific, Indian Ocean, South Atlantic, or South Pacific subtropical gyre regions. There was a focus on adding the flux into subtropical gyres, as the centre of these gyres are convergence zones due to Ekman transport and result in greater plastic accumulation (Eriksen *et al.,* 2019). The size and location of the subtropical gyres, into which the DIC flux was added, were estimated from Figure 2.1 and illustrated in Figure 3.1.

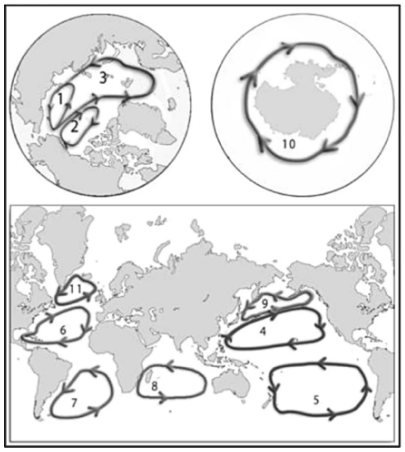

Figure 2.1. Location of the world's 11 oceanic gyres. Reproduced from Eriksen *et al.,* (2019) and originally adapted from Ebbesmeyer & Scigliano, (2010). Gyres numbered 4 – 8 were used as a template to approximate the area into which the plastic-derived DIC flux was added.

Model runs PROJ-NA-500 and PROJ-SA-500 included a projected plastic-derived DIC flux which was added to the North Atlantic (PROJ-NA-500) and South Atlantic (PROJ-SA-500) subtropical gyre regions over 500 years. These model runs were completed to determine whether a greater period of additional oceanic DIC input would create more negative effects on Earth's climate system. Finally, runs PROJ-COA and PROJ-COA-500 included a projected plastic-derived DIC flux which was distributed evenly along the global coast for 100 and 500 years respectively. Model runs PROJ-COA and PROJ-COA-500 included a projected plastic-derived DIC flux which was added to ocean grid cells adjacent to the entire global coastline as the majority of marine plastic pollution accumulates on shorelines (Eunomia, 2016).

Chapter 3: Modelling Results

All results displayed in this chapter are not the total concentration of the specified tracers but differences from the control integration. Differenced global oceanic DIC concentrations after the input of the projected plastic-derived DIC flux for 10 years, are shown in Figure 3.1.

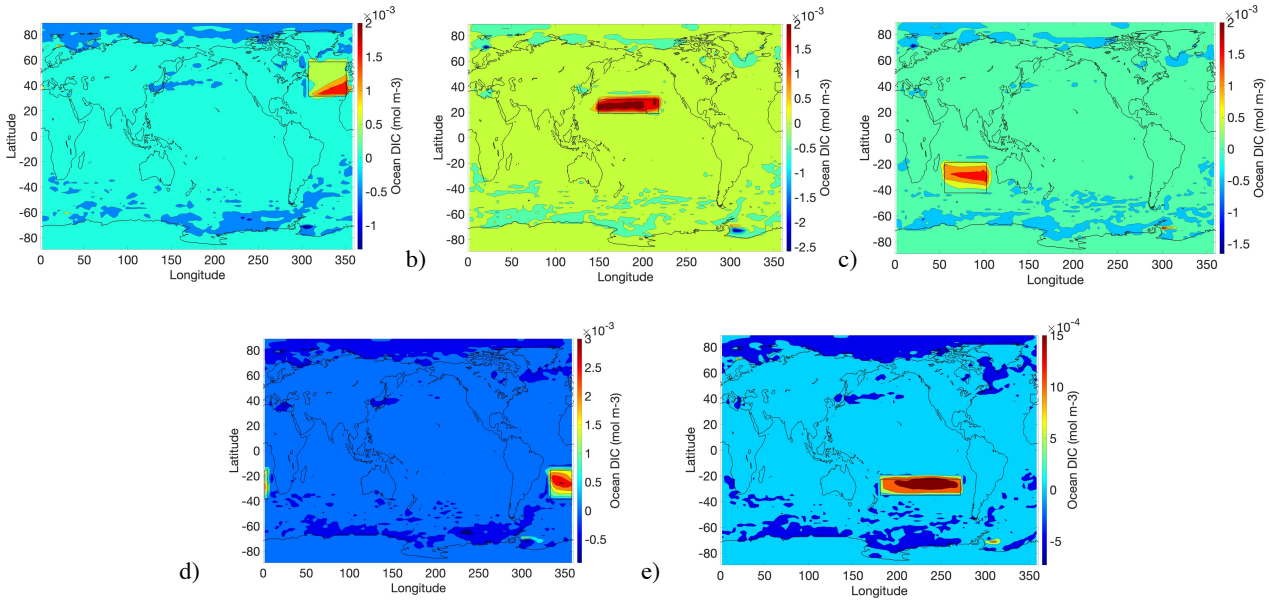

Figure 3.1. Differenced global oceanic surface DIC concentrations (mol m^{-3}) at 17.5m depth after the addition of a DIC flux (based on projected values of marine plastic) into the **a)** North Atlantic, **b)** North Pacific, **c)** Indian Ocean, **d)** South Atlantic, and **e)** South Pacific subtropical gyres, after 5 years of integration. The locations of flux input are illustrated with a black box. These model results represent a 10-year average centred around 2005. Values display the difference from those of the control integration and were averaged and recorded every 10 years.

These DIC concentrations were averaged over the first 10 years of the 100-year integration and centred around year 5. Each panel represents a different location into which the flux was added. DIC concentrations increased where the flux was initially added, with levels decreasing further away from the centre of these areas. In the areas that experienced the addition of plastic-derived DIC fluxes, the greatest increase in DIC concentrations was found in the South Atlantic Ocean at 3.12 x 10^{-3} mol m^{-3} and the smallest increase was in the Indian Ocean, at 1.80 x 10^{-3} mol m^{-3}. There were other regions near the Arctic and Antarctic, which displayed increases in DIC concentrations, however, these regions were not in close proximity to the areas of initial input. The oceanic DIC concentrations in the control integration ranged from 1.88 to 2.44 mol m^{-3} throughout the entire integration period. The greatest increase in DIC concentrations after ~5

years of integration (3.12 x 10^{-3} mol m^{-3} in the South Atlantic) was 0.56% of the greatest increase observed in the control integration.

Differenced global oceanic DIC concentrations, after the input of the projected plastic-derived DIC flux for 100 years, are shown in Figure 3.2. These DIC concentrations were averaged over the last 10 years of the 100-year integration and represent an average centred around year 2095. Differenced DIC concentrations decreased around the area of the initial flux input but were generally still greater than 0 around this area, versus other regions. Near the boxed areas of input, the greatest increase in DIC concentrations occurred after the input of the flux into the North Atlantic Ocean, at 2.18 x 10^{-3} mol m^{-3}. The smallest increase remained in the Indian Ocean at 9.48 x 10^{-4} mol m^{-3}. These differences may be attributed to the rates of CO_2 uptake in different ocean basins and will be described in further detail in the Discussion section (under Atmospheric CO_2 Concentrations) of this thesis. In some experiments, there were other regions with greater increases in DIC concentrations that were not in close proximity to the areas of initial input. The greatest increase in DIC concentrations after ~95 years of integration (1.81 x 10^{-3} mol m^{-3}) was 0.39% of the increase observed in the control integration.

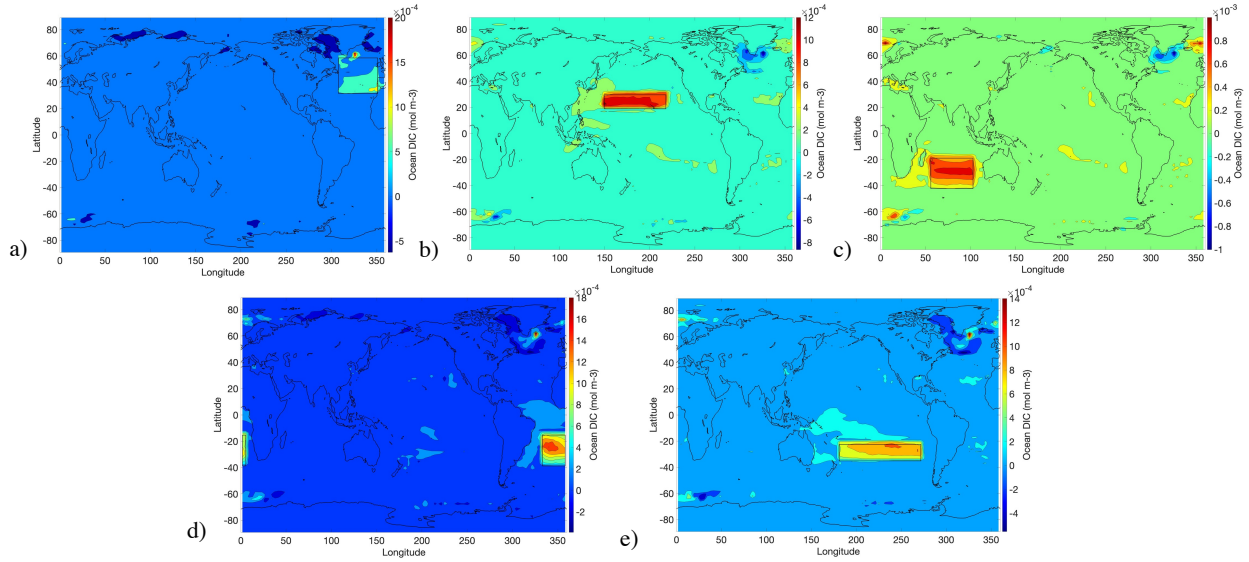

Figure 3.2. Differenced global oceanic surface DIC concentrations (mol m^{-3}) at 17.5m depth after the addition of a DIC flux (based on projected values of marine plastic) into the **a)** North Atlantic, **b)** North Pacific, **c)** Indian Ocean, **d)** South Atlantic, and **e)** South Pacific subtropical gyres, after 95 years of integration. The locations of flux input are illustrated with a black box. These model results represent a 10-year average centred around 2095. Values in the above plots are the difference from those of the control integration and were averaged and recorded every 10 years.

Illustrated in Figure 3.3 are the differenced and globally averaged oceanic DIC concentrations after the input of the projected plastic-derived DIC flux into various regions of the ocean, over 100 years of integration. DIC concentrations gradually increased throughout the integration, with the greatest increase of 3.83×10^{-5} mol m^{-3}, occurring after the flux was added into the North Atlantic Ocean (Figure 3.3a). The smallest increase was observed after the flux was added to the Indian Ocean. Generally, all trend lines remained close in range in the beginning and became more different as time progressed. There is a difference between these values and those of the control integration, which gradually increased from 2.29 to 2.32 mol m^{-3} throughout the 100-year integration. The greatest increase in DIC concentrations throughout the 100-year integration (3.83×10^{-5} mol m^{-3}) was 0.13% of the increase in the control integration.

Figure 3.3b displays an overall increase in surface ocean DIC concentrations over the 100-year period. The greatest increase, of 1.95×10^{-4} mol m^{-3}, occurred after the flux was distributed along the global coast. The maximum increase occurred in 2036 and then plateaued until the end of the integration. These values should be compared to those of the control integration, which gradually increased from 2.06 to 2.19 mol m^{-3} throughout the 100-year period. The greatest increase in surface ocean DIC concentrations throughout the 100-year integration (1.95×10^{-4} mol m^{-3}) was 0.15% of the increase in the control integration.

Figure 3.3c displays the overall decrease in the DIC flux rate over the 100-year integration. Although the DIC flux rates were greater than the control, because of the plastic-derived DIC flux input, the plot illustrates decreasing rates as time progressed. The difference in flux rate values was initially positive at an average of 1.48×10^{-10} mol m^{-2} s^{-1} and although rates decreased throughout the 100-year period, the average flux rate was positive in 2100. The greatest decrease in the oceanic DIC flux rate, at -1.05×10^{-11} mol m^{-2} s^{-1}, occurred after the flux was added into the South Pacific Ocean. All trend lines remained in a similar range throughout the integration. The above values can be compared to the control integration which increased from 1.64×10^{-8} to 3.97×10^{-8} mol m^{-2} s^{-1}. The greatest decrease in the globally averaged DIC flux rates throughout the 100-year integration (-1.05×10^{-11} mol m^{-2} s^{-1}) was 0.05% of the increase in the control integration.

a)

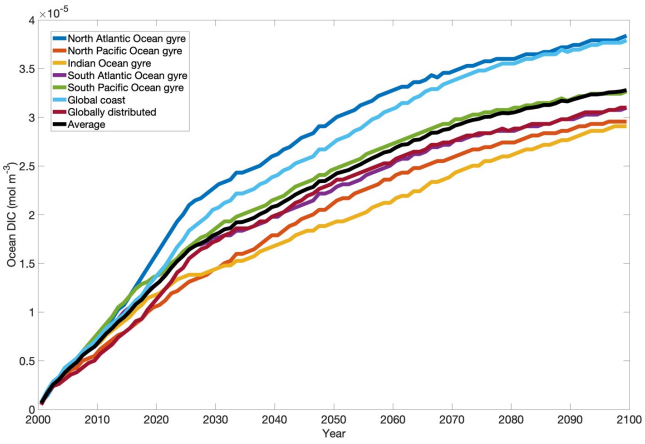

b)

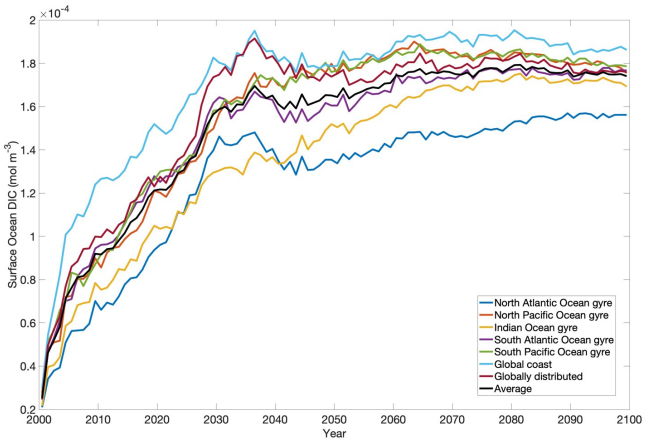

c)

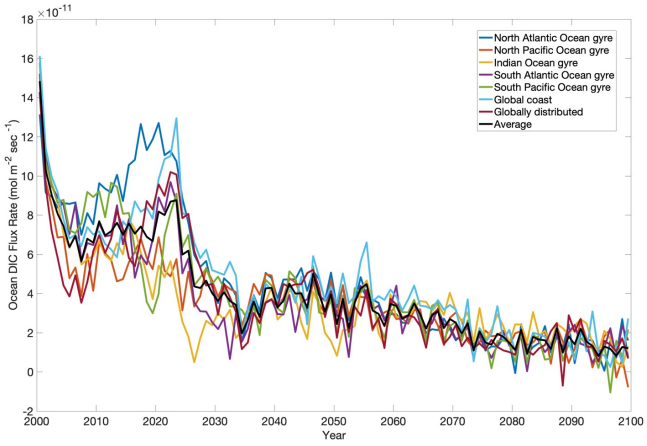

Figure 3.3. Differenced oceanic DIC concentrations after the input of an oceanic DIC flux, based on projected marine plastic values, after 100 years of integration. This figure displays **a)** globally averaged DIC concentrations (mol m^{-3}), **b)** globally averaged DIC concentrations in the surface ocean (mol m^{-3}), and **c)** globally averaged oceanic DIC flux rates (mol m^{-2} s^{-1}). Values and rates in the above plots display the difference from those of the control integration and were averaged and recorded annually.

Figure 3.4 displays globally averaged atmospheric CO_2 concentrations after the input of the projected plastic-derived DIC flux into various regions of the ocean, over 100 years of

integration. The greatest increase in atmospheric CO_2, of 1.08 ppm, occurred after the input of the flux into the North Pacific Ocean. There was a minor decrease in atmospheric CO_2 concentrations in ~2025, but generally, a gradual increase was observed. All trend lines remained in a similar range throughout the integration. It is important to compare these values to those of the control integration which gradually increased from 365.7 to 930.4 ppm over the 100-year period. The greatest increase in globally averaged atmospheric CO_2 concentrations throughout the 100-year integration (1.08 ppm) was 0.19% of the increase in the control integration.

Figure 3.4b displays the comparison of current versus projected globally averaged atmospheric CO_2 concentrations, after the flux was distributed throughout the global ocean over the 100-year period. The results illustrate greater atmospheric CO_2 concentrations when the projected plastic-derived DIC flux was added. Like the results in Figure 3.4a, atmospheric CO_2 concentrations, based on both current and projected DIC flux values, experienced a minor increase in ~2025. The greatest increase was observed after the input of the projected flux, at 1.07 ppm, at the end of the integration. This increase was greater by 0.6 ppm, than after the input of the current flux, which reached a maximum of 0.47 ppm in 2100.

Figure 3.4c displays the globally averaged atmospheric CO_2 values after the input of the projected plastic-derived DIC flux into the North and South Atlantic Ocean as well as the global coast, after 500 years of integration. The greatest increase in concentrations throughout the integration occurred after the input of the flux into the South Atlantic Ocean (6.20 ppm). The smallest increase occurred when the flux was added into the North Atlantic Ocean (6.05 ppm). It is important to compare these values to those of the control integration, which gradually increased from 366 to 1.97×10^1 ppm over the 500-year period. When comparing these runs every 100 years, there was a greater increase in atmospheric CO_2 values over the 500-year period versus the increase observed at the end of the 100-year integration (Figure 3.4a). The greatest increase in globally averaged atmospheric CO_2 concentrations throughout the 500-year integration (6.20 ppm) was 0.38% of the increase in the control integration.

When observing the pattern in atmospheric CO_2 after the addition of the plastic-derived DIC flux, there were very minor increases in concentrations after the input of both the current and projected plastic-derived DIC flux, regardless of the location of input or period of integration. A minor increase in values occurred after ~20 years of integration throughout these model runs.

a)

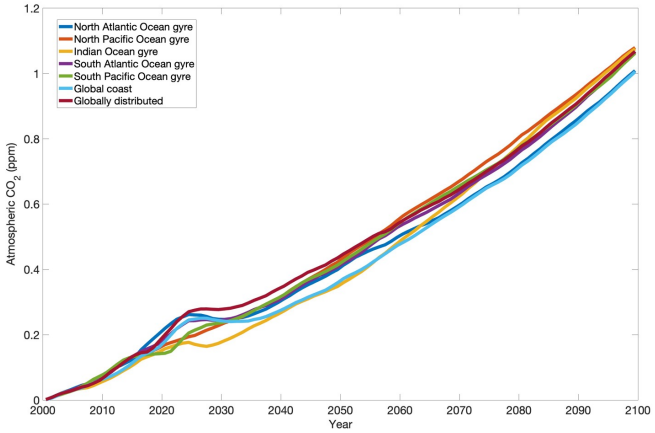

b)

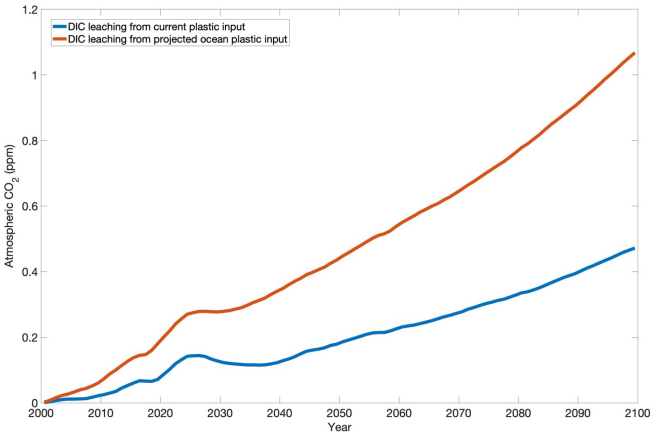

c)

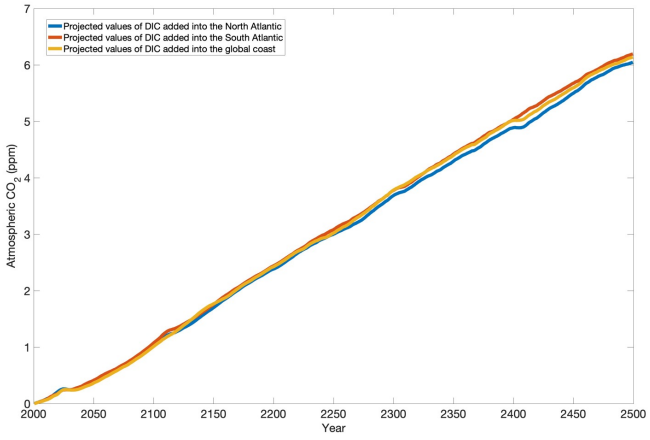

Figure 3.4. Differenced and globally averaged atmospheric CO_2 concentrations (ppm) after the input of an oceanic DIC flux based on **a)** projected marine plastic values into various regions of the ocean, after 100 years of integration. This figure also displays **b)** current versus projected marine plastic values, distributed evenly into the global ocean after 100 years of integration, as well as **c)** after the input of the DIC flux based on projected values over 500 years of integration. Values in the above plots display the difference from those of the control integration and were averaged and recorded annually.

Figure 3.5 shows surface air temperature (SAT) after the input of the projected plastic-derived DIC flux into various locations of the global ocean, over 100 years of integration. Figure 3.5a displays an increase in globally averaged SAT with the greatest increase in temperatures, at 0.0118°C in 2015, occurring after the distribution of the flux across the global ocean. This was followed by an increase of 0.0116°C, after the flux was added into the North Atlantic Ocean. All values remained within the same range throughout the 100-year integration and experienced only minor fluctuations. It is important to compare these values to those of the control integration, which gradually increased from 14.0 to 17.6°C, over 100 years of integration. The greatest increase in globally averaged atmospheric CO_2 concentrations throughout the 500-year integration (0.0118°C) was 0.33% of the increase in the control integration.

Figure 3.5b displays the global distribution of SAT after the input of the plastic-derived DIC flux into the North Atlantic Ocean, after 15 years of integration. This point in time was chosen to be included in the results as it displays the greatest increase in SAT throughout the 100-year period, at 0.15 °C. This greatest increase was located at 72.9°N, 16.2°E. Although all regions experienced very minor warming as a result of the addition of the DIC flux into the North Atlantic Ocean, the greatest warming was illustrated in the Arctic region.

Figure 3.5c displays the global distribution of SAT after the input of the plastic-derived DIC flux into the North Atlantic Ocean, after 95 years of integration. In general, the increase in SAT over the Northern Hemisphere was greater than that of the Southern Hemisphere. A decrease in SAT was observed in a few regions of the Southern Hemisphere. The greatest increase, of 0.016°C, occurred at 62.1°, 325.8°. There was a greater increase in SAT after 15 years of integration versus after 95 years of integration.

When observing the overall pattern in SAT as a result of the plastic-derived DIC flux input, there was a very minor increase in temperatures, regardless of the location of the input. The northern hemisphere region, and more specifically the Arctic, experienced the greatest warming.

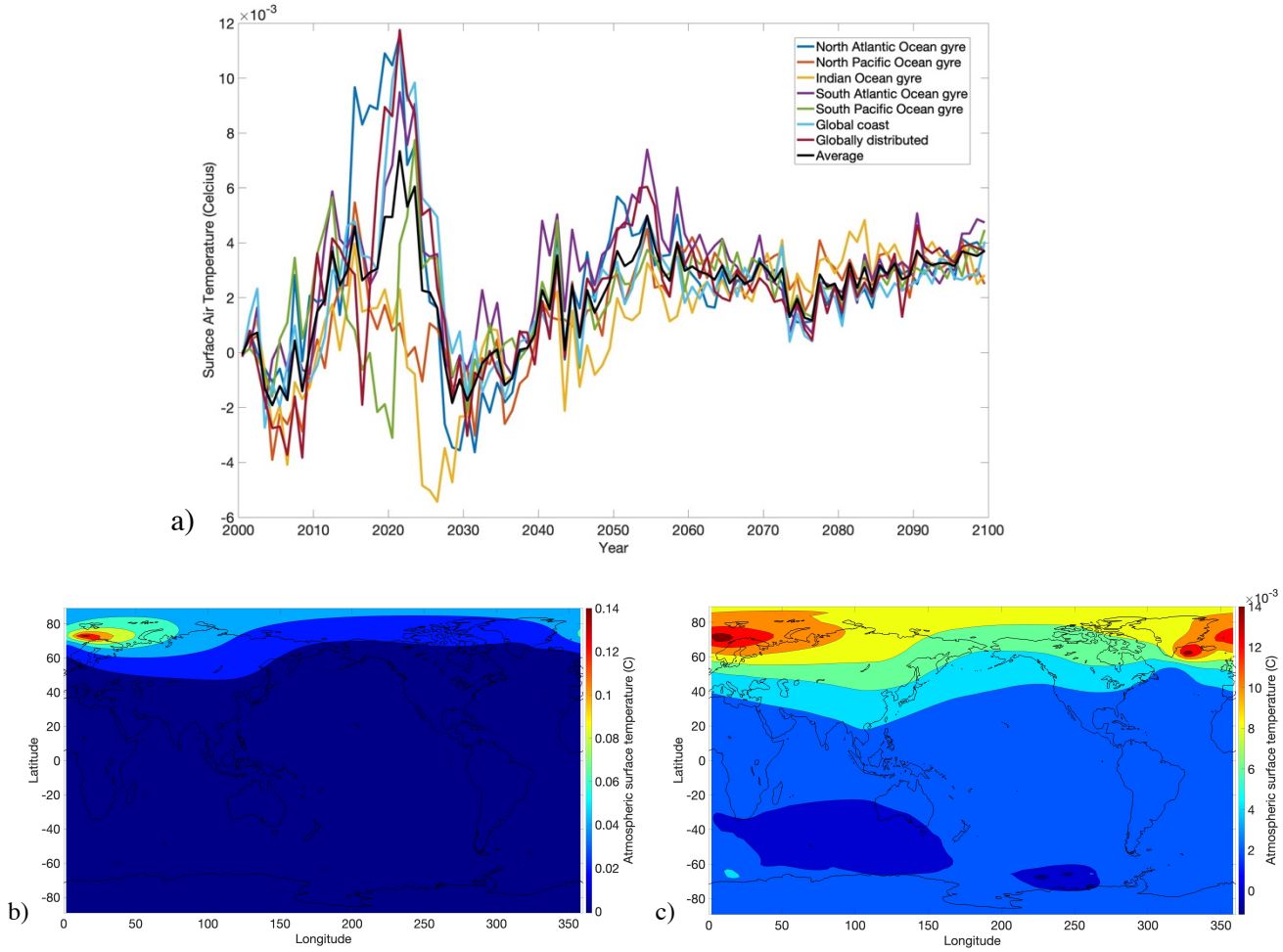

Figure 3.5. Differenced surface air temperatures after the input of an oceanic DIC flux, based on projected marine plastic values. This figure displays **a)** globally averaged SAT values (°C) for 100 years of integration, averaged and recorded annually, **b)** global distribution of SAT after the input of the DIC flux into the North Atlantic Ocean gyre representing a 10-year average centred around 2015, and **c)** global distribution of SAT after the input of the DIC flux into the North Atlantic Ocean, representing a 10-year average centred around 2095. Values in the above plots display the difference from those of the control integration.

Figure 3.6 displays globally averaged ocean temperatures after the input of the projected plastic-derived DIC flux into various regions of the ocean, over 100 years of integration. Figure 3.6a shows an overall increase in ocean temperatures, which reached a maximum of 5.99 x 10^{-4} °C, after the input of the flux into the North Pacific Ocean. The temperature values of all trend lines were in a similar range near the beginning of the integration and became more different as time progressed. The above values are evidently smaller than those of the control integration

which gradually increased from 3.80 to 4.36°C over the 100-year period. The greatest increase in globally averaged ocean temperatures throughout the 100-year integration (5.99 x 10^{-4} °C) was 0.11% of the increase in the control integration.

a)

b)

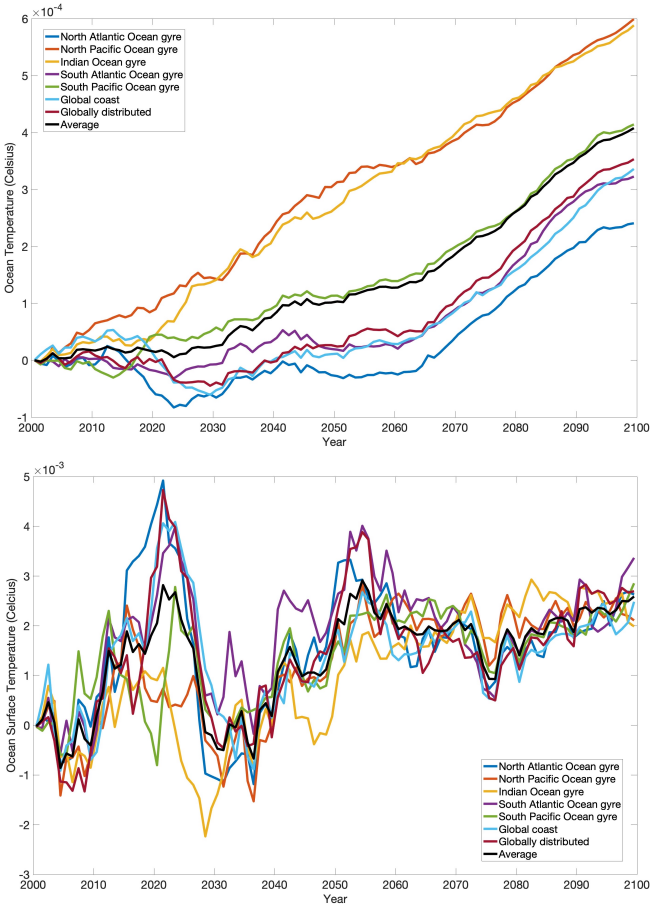

Figure 3.6. Differenced ocean temperatures (°C) after the input of an oceanic DIC flux, based on projected marine plastic values, after 100 years of integration. This figure displays **a)** globally averaged ocean temperatures, and **b)** globally averaged surface ocean temperatures. Values in the above plots display the difference from those of the 100-year control integration and were averaged and recorded annually.

Figure 3.6b displays an overall increase in surface ocean temperatures, with the greatest increase (4.92 x 10^{-3}°C) occurring after the addition of the flux into the North Atlantic Ocean. This increase occurred after ~20 years of integration. Although all trend lines fluctuated throughout the 100-year period, they remained within a similar range throughout the integration. The values of the control integration, which gradually increased from 18.4 to 20.9°C over the 100-year period, should be compared to the temperatures stated above. The greatest increase in

globally averaged surface ocean temperatures throughout the 100-year integration (4.92 x 10^{-3}°C) was 0.20% of the increase in the control integration.

When observing the overall pattern in ocean temperatures as a result of the plastic-derived DIC flux input, there was a very minor increase in globally averaged ocean temperatures, regardless of the location of the input.

Figure 3.7 displays globally averaged ocean surface pH levels after the input of the plastic-derived DIC flux into various regions of the global ocean, over 100 years of integration. This figure displays an overall decrease in differenced pH levels, with trend lines remaining in a similar range throughout the integration. The distribution of the flux along the global coast yielded the greatest decrease of 5.57 x 10^{-4} pH units. The smallest decrease occurred after the input of the flux into the North Atlantic Ocean. The values of the control integration which decreased from 8.08 to 7.72 pH units over the 100-year period, are evidently greater than those stated above. The greatest decrease in globally averaged pH levels throughout the 100-year integration (-5.57 x 10^{-4} pH units) was 0.15 % of the decrease in the control integration.

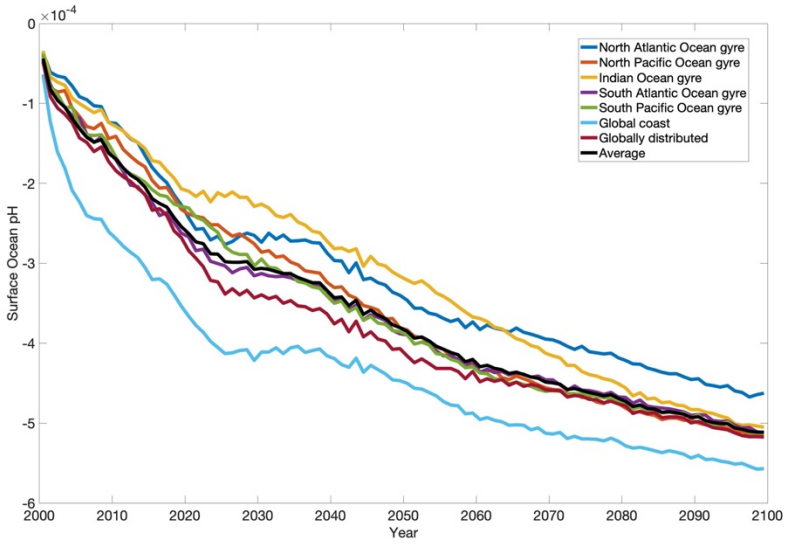

Figure 3.7. Differenced and globally averaged oceanic pH levels after the input of an oceanic DIC flux, based on projected marine plastic values, after 100 years of integration. Values in the above plots display the difference from those of the 100-year control integration and were averaged and recorded annually.

Globally averaged ocean alkalinity concentrations generally remained the same after the addition of the plastic-derived DIC flux. It is important to note that the control integration also generally remained the same, with a very minor decrease from 2.4205 to 2.4203 mol m^{-3} over the

100-year period. Figure 3.8 displays a very minor decrease in surface ocean alkalinity concentrations and with the greatest decrease, of -2.60 x 10^{-5} mol m^{-3}, occurring after the input of the flux into the North Atlantic Ocean. Differences in concentrations increased ~2038, and fluctuated for the rest of the integration. Generally, all trend lines remained within a similar range throughout the 100-year period. These values can be compared to those of the control integration, which decreased from 2.34 to 2.32 mol m^{-3} throughout the 100-year period. The greatest decrease in globally averaged surface alkalinity concentrations throughout the 100-year integration (-2.60 x 10^{-5} mol m^{-3}) was 0.13% of the decrease in the control integration.

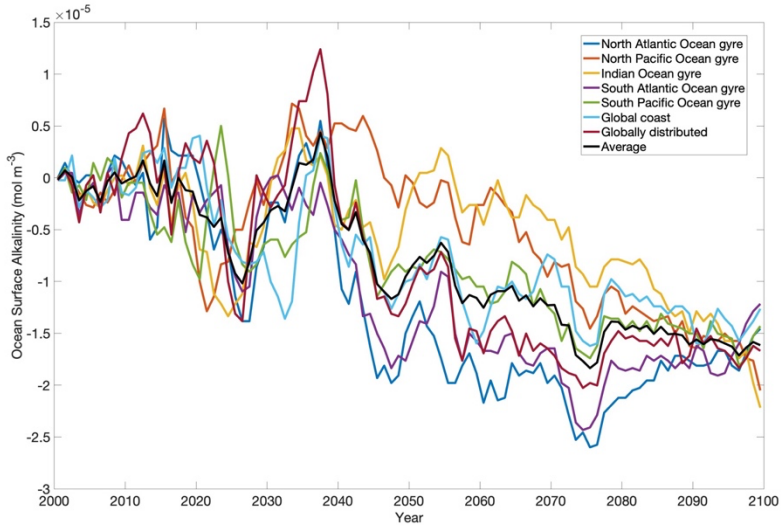

Figure 3.8. Differenced and globally averaged surface ocean alkalinity (mol m^{-3}) after the input of an oceanic DIC flux, based on projected marine plastic values, after 100 years of integration. Values in the above plot display the difference from those of the 100-year control integration and were averaged and recorded annually.

Figure 3.9 displays globally averaged oceanic oxygen concentrations after the input of a projected plastic-derived DIC flux into various regions of the global ocean, over 100 years of integration. Figure 3.9a displays an overall decrease in oceanic oxygen concentrations which reached a minimum of -9.46 x 10^{-6} mol m^{-3} and occurred after the input of the flux into the North Pacific Ocean. Concentrations briefly increased in ~2020 and again in ~2040, and experienced fluctuations throughout the integration. Generally, all values remained in a similar range near the beginning of the integration and became more different as time progressed. The control integration, which gradually decreased from 0.174 to 0.167 mol m^{-3} over the 100-year period, can be compared to the concentrations mentioned above. The greatest decrease in globally

averaged surface oxygen concentrations throughout the 100-year integration -9.46 x 10^{-6} mol m^{-3}) was 0.14% of the decrease in the control integration.

a)

b)

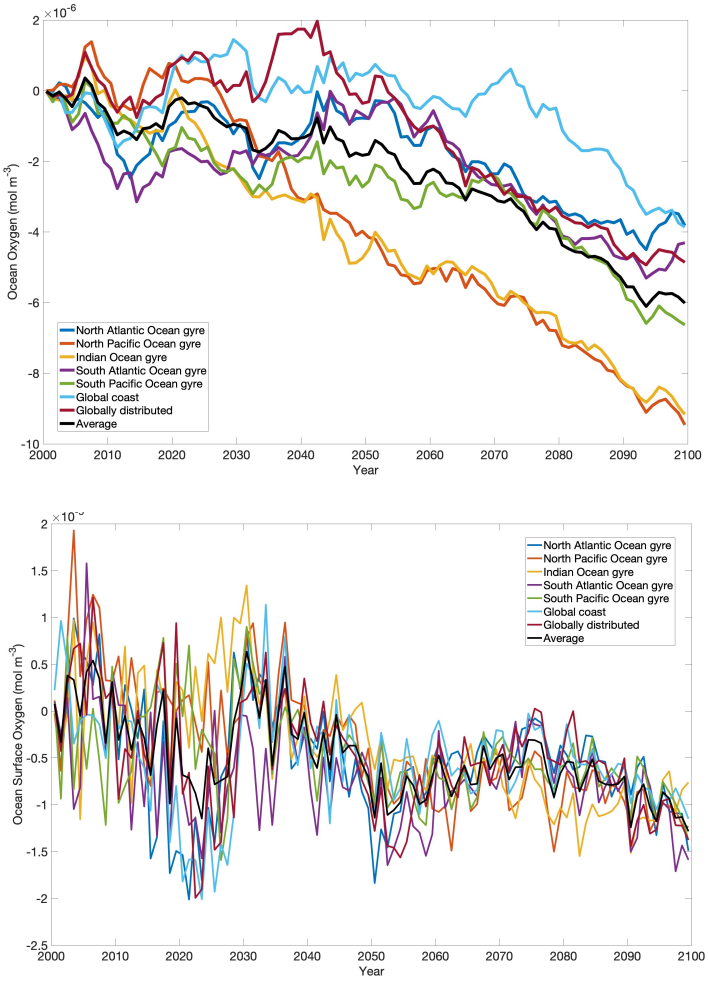

Figure 3.9. Differenced oceanic oxygen concentrations (mol m^{-3}) after the input of an oceanic DIC flux, based on projected marine plastic values, after 100 years of integration. **a)** Globally averaged oceanic oxygen concentrations; **b)** globally averaged surface ocean oxygen concentrations. Values in the above plots display the difference from those of the 100-year control integration and were averaged and recorded annually.

Figure 3.9b illustrates an overall decrease in globally averaged surface ocean oxygen concentrations which reached a minimum of -2.01 x 10^{-5} mol m^{-3} after the flux was added to the South Atlantic Ocean for the 100-year period. Surface ocean oxygen concentrations remained within a similar range throughout the entire integration. The values of the control integration, which gradually decreased from 0.246 to 0.236 mol m^{-3} over the 100-year integration, are greater than the differences in concentrations stated above. The greatest decrease in globally averaged

surface ocean oxygen concentrations throughout the 100-year integration (-2.01 x 10^{-5} mol m^{-3}) was 0.20% of the decrease in the control integration. There was only a very minor decrease in oxygen concentrations, regardless of the location of plastic-DIC flux input.

Figure 3.10 displays the maximum Atlantic meridional overturning circulation (AMOC) index after the input of the projected plastic-derived DIC flux into various regions of the global ocean, throughout 100 years of integration. The AMOC index is an indicator of the overall strength of the AMOC and is defined here to be the maximum Atlantic meridional overturning streamfunction in the Atlantic below 200m depth and between 20°N and 70°N.

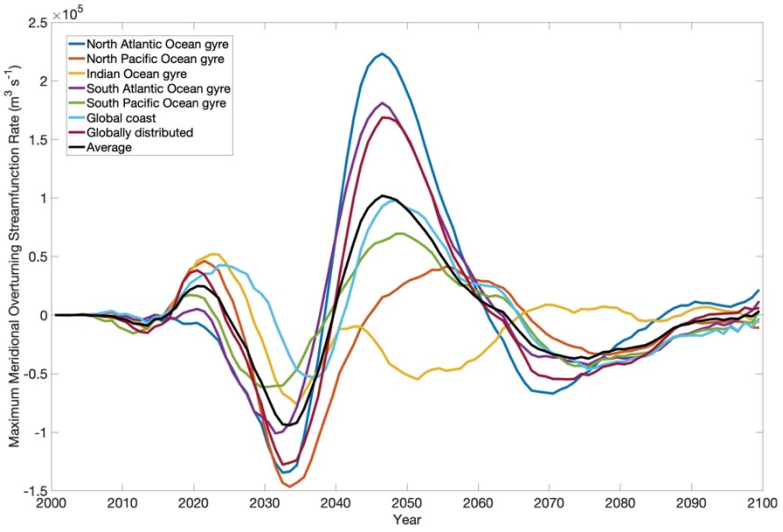

Figure 3.10. Differenced maximum Atlantic meridional overturning circulation index (m^3 s^{-1}) after the input of an oceanic DIC flux, based on projected marine plastic values, after 100 years of integration. Rates in the above plot display the difference from those of the 100-year control integration and were averaged and recorded annually.

There was an overall decrease in the AMOC index with the greatest decrease occurring in 2031, at -1.47 x 10^5 m^3 sec^{-1}, after the flux was added into the North Pacific Ocean. The greatest increase of 2.79 x 10^5 m^3 sec^{-1}, occurred in 2046 after the flux was added into the North Atlantic Ocean. The trend lines observed in Figure 3.10 fluctuated throughout the integration, whereas the control integration experienced a gradual decrease from 1.97 x 10^7 to 1.32 x 10^7 m^3 sec^{-1}. The greatest decrease in the globally averaged AMOC index throughout the 100-year integration (-1.47 x 10^5 m^3 sec^{-1}) was 2.26% of the decrease in the control integration.

Figure 3.11 illustrates the mass of globally averaged land soil carbon after the input of the projected plastic-derived DIC flux into various regions of the global ocean, over 100 years of

integration. These trend lines were similar at the beginning and the end of the integration but showed some variation between. The greatest increase, of 0.39 kg, occurred after the input of the flux into the Indian Ocean. After 15-25 years of integration, all trend lines experienced a decrease with the greatest being -0.19 kg, after the flux was added into the North Atlantic. It is important to compare these values to those of the control integration, which gradually increased from 1.23 x 10^3 to 1.29 x 10^3 kg throughout the 100-year period. The greatest increase in globally averaged land soil carbon throughout the 100-year integration (0.39 kg) was 0.62% of the increase in the control integration.

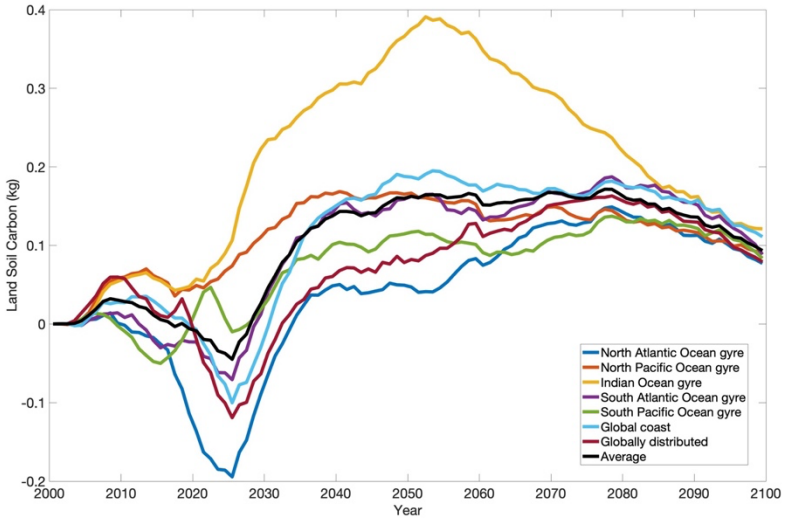

Figure 3.11. Differenced and globally averaged land soil carbon (kg) after the input of an oceanic DIC flux, based on projected marine plastic values, after 100 years of integration. Values in the above plot display the difference from those of the 100-year control integration and were averaged and recorded annually.

Although there are both increases and decreases in oceanic and atmospheric tracers as a result of the input of the plastic-derived DIC flux, when comparing these values to those of the control run, the resultant change is very minor. All model variables changed by less than 1% from the control; the change in the AMOC index was 2.26% of the control. In general, differenced values in tracers as a result of the DIC flux input followed the same pattern of increase or decrease as those of the control run. For example, if the control run values increased throughout the integration, the differenced values as a result of the flux input also increased throughout the integration.

Chapter 4: Discussion

As marine plastic pollution enters the marine environment, it leaches labile DOC which is rapidly broken down by biota into inorganic carbon (Romera-Castillo *et al.,* 2018). Several scientific studies have discussed the concerns with having additional sources of carbon enter the ocean and how this could impact microbial communities, carbon sequestering blue carbon ecosystems, and one of the greatest concerns being the effects on atmospheric CO_2 levels. A major concern in science and society today is the effect that large amounts of greenhouse gas emissions released into the atmosphere, resulting from anthropogenic activities, are having on Earth's climate system. The largest contributions include energy-related emissions from the generation of electricity, heat, and transport across various industries (IPCC, 2021). These activities are leading to rising atmospheric and oceanic temperatures, glacial retreat, sea level rise, increases in the frequency and intensity of precipitation events, extreme heatwaves, and agricultural and ecological droughts, amongst others (IPCC, 2021). As stated in the IPCC's sixth assessment report, "Human influence has warmed the climate at a rate that is unprecedented in at least the last 2000 years". In 2019, atmospheric CO_2 concentrations were at their highest within the last 2 million years and have increased by 47% since 1750 (IPCC, 2021).

Marine plastic pollution is another potentially severe anthropogenic-induced issue that can threaten several marine ecosystems. This can occur through the emissions of CO_2 and harmful gases during the production and incineration of plastic, the damage to the physical and reproductive health of organisms, the transport of invasive species, the social and economic consequences of blockages and accumulation, and the leaching of compounds into the marine environment. Given the urgency and consequential effects of global warming, it is important to fully explore all CO_2-emitting anthropogenic activities and study how they are impacting the natural environment. Therefore, it was important to analyze the carbon-leaching element of marine plastic pollution and determine whether it is significantly harmful to Earth's climate. The results of this study, however, indicate that very minor changes occur in atmospheric and oceanic tracers, and ultimately our climate system, as a result of plastic-derived carbon leaching.

4.1 DIC Concentrations

DIC moves with surface currents, driven by global wind systems, which are fueled by solar energy. Density differences, resulting from temperature and salinity variations in water

masses, result in the rising of warmer, less saline water, and the sinking of colder, more saline water; this process forms part of the thermohaline circulation. Finally, motion associated with tides near shorelines creates ebb currents and flood currents; ebb currents correspond to landward flow, while flood currents correspond to seaward flow. In addition, the vertical movement of water is determined by upwelling and downwelling, whereby the water level is lowered or elevated as a result of the divergence and convergence of ocean currents, respectively.

In this study, although DIC concentrations were added to specified regions of the ocean, through all of the above-mentioned processes, DIC dispersed outside each grid box over time. Generally, however, the greatest increases in DIC concentrations remained near the areas of initial input. These changes in DIC concentrations are especially evident when comparing the 5- and 95-year integration. At the end of the integration, there was less DIC present at 17.5m depth than was initially added into each grid box of the model. This can be attributed to the decrease in solubility of CO_2 in the surface ocean as temperatures rise towards the end of the control integration; this principle will further be discussed in this subsection. When observing the globally averaged DIC concentrations, however, there was an overall increase. Although the concentrations of DIC at the initial point of entry decreased, additional DIC was consistently being added into the ocean through plastic-derived carbon leaching, and so the overall concentration increased. The increase in DIC as a result of the leaching is very minor; this is especially evident when we compare the greatest increase of 3.84×10^{-5} mol m^{-3} to the average concentration of DIC in ocean water which is 2.4 millimoles (Yan *et al.,* 2020) or 2.4×10^{-3} mol. Other than the location of initial DIC input, other regions of DIC increase occurred in the Arctic and Antarctic regions. This may be indicative of the location of polynyas (an area of open water surrounded by sea ice) occurring in this region, rather than the transport of the DIC from the initial area of input, as thermohaline circulation transports tracers on very long time scales and these integrations were only 100 years long. These regions experience an enhanced vertical carbon flux which may explain the increased presence of DIC (Grebmeier & Barry, 2007).

Naturally, oceanic DIC is 10-15% higher in deep waters versus surface waters (Feely *et al.,* 2001), as organisms die, sink, and decompose. In the current study, the results indicate that relative to the control run, surface ocean DIC concentrations were greater than those in deeper waters. Of course, this reflects the fact that the DIC flux was added to the surface ocean in the

perturbation experiment. The DIC flux rate decreased over time, even though the flux being added into the surface ocean remained the same throughout the integration. As atmospheric CO_2 concentrations increase, so does SAT. In accordance with Le Chatelier's principle, the system adjusts for the excess heat in the atmosphere by introducing more heat into the ocean and inhibiting the dissolution of CO_2 (Lu *et al.,* 2017). This results in lower concentrations of CO_2 being found in the surface ocean, and ultimately, a lower flux rate.

4.2 Atmospheric CO_2 Concentrations

Through the process of air-sea gas exchange, CO_2 is transferred across the air-water interface and is controlled chemically, by the CO_2 concentration gradient, and physically, by turbulence and molecular diffusion (Likens, 2009). In the model, some of the plastic-derived DIC in the ocean entered the atmosphere via this exchange and ultimately resulted in increased concentrations of atmospheric CO_2. The greatest increase, throughout the 100-year period, that resulted from plastic-derived carbon leaching, was 1.08 ppm, which is very minor when compared to the current annual rise of 2.4 ppm (Friedlingstein, 2022). The greatest increases occurred after the flux was added into the North Pacific Ocean and the Indian Ocean. Takahashi *et al*., (1997) found that the Pacific Ocean, Southern Ocean, and the Indian Ocean take up the least CO_2, while the Atlantic Ocean takes up the most (Takahashi *et al.,* 1997). This could be explained by the presence of the overturning circulation in the Atlantic Ocean, where deep water formation occurs, and surface CO_2 is brought down into deeper waters. Atmospheric CO_2 concentrations based on projected marine plastic values are visibly greater than those based on current values. This is expected as annual concentrations of projected marine plastic are set to increase with time (12.7 million metric tonnes year $^{-1}$ to 29 million metric tonnes year $^{-1}$). As plastic-carbon leaching occurred for a longer period of time (500 years), this slightly amplified the effects on atmospheric CO_2 concentrations. After 500 years of plastic-derived carbon leaching, the centennial increase in concentrations became greater as time progressed, resulting in an overall increase of 6.20 ppm by 2500.

4.3 Surface Air Temperatures (SAT)

Through the greenhouse effect, as atmospheric CO_2 concentrations increase, longwave radiation emitted from the Earth's surface becomes trapped in the atmosphere, resulting in

atmospheric warming. This warming is leading to global mean sea level rise through ice loss and thermal expansion, an increase in the frequency and intensity of hot extremes and heavy precipitation, increased occurrence of marine heatwaves, an increase in temperature of the coldest days in the Arctic, permafrost thawing, loss of snow cover, amongst other changing conditions (IPCC, 2021). In the model, as carbon enters the ocean from plastic-derived carbon leaching (in the form of DIC), it eventually enters the atmosphere through air-sea exchange and contributes to rising SAT. The global average increase in temperature, from plastic-derived carbon leaching, was very minor at 0.0118°C, and is especially small when compared to the observed warming of 1.59°C over land since pre-industrial times (IPCC, 2021).

Increases in SAT varied regionally, with the Arctic warming much faster than other regions of the world; this occurs since there increased absorption of solar radiation by the land and ocean which is becoming exposed as ice melts due to ice-albedo feedback (Dai *et al.,* 2019; Rantanen *et al.,* 2022). The results of the present study displayed the greatest increase in global mean temperatures occurring in the Arctic region after the input of the plastic-derived DIC flux. The increase in temperatures became larger with increasing latitudes; typically referred to as polar amplification. Small regions in the Arctic and Antarctic display increases in DIC concentrations, which may also be explained by the occurrence of polynyas as described in the DIC concentrations subsection in the Results section of this thesis. As regions of ocean surface within polynyas have a reduced albedo, they absorb increased shortwave solar radiation and so the temperature in that area is greater (Weijer *et al.,* 2017).

4.4 Ocean Temperatures

With an increase in SAT, ocean water temperatures are rising. Although ocean basins have a low albedo and are good absorbers of incoming solar radiation, water has a high heat capacity, meaning ocean temperatures are rising more slowly than land temperatures (IPCC, 2021). As a result of the increase in atmospheric CO_2 concentrations, and the resultant rise in SAT, global oceanic temperatures have increased by 0.88°C from 2011-2020 compared to 1850-1900 (IPCC, 2021). With the input of the plastic-derived DIC flux, globally averaged ocean temperatures increased by 5.99×10^{-4}°C throughout the 100-year period. This rise is minimal when compared to the projected annual increase in ocean temperatures of 1.2°C – 3.2°C by 2100 (IPCC, 2021), and will not significantly contribute to the effects of rising ocean temperatures

which include sea ice melt, marine heatwaves, coral bleaching, and loss of breeding grounds for marine organisms (IPCC, 2021). Ocean temperatures are greatest at the surface as solar radiation is unable to penetrate deeper waters. This is consistent with the results of this study which display greater increases in surface ocean temperatures by one order of magnitude when compared to the increase observed in average ocean temperatures.

4.5 Ocean pH

As previously mentioned in the introductory section of this thesis, atmospheric CO_2 concentrations are contributing to the acidification of ocean waters. Greater concentrations of CO_2 result in an increase in H^+ as CO_2 and H_2O form H_2CO_3, and this weak acid dissociates into H^+ and HCO_3^-. Greater H^+ concentrations will bond with CO_3^{2-} (forming HCO_3^-) and will inhibit the formation of $CaCO_3$. The acidification of waters, observed as a result of anthropogenic CO_2 emissions, impacts carbon fixation rates of photosynthesizing organisms, oceanic biogeochemical cycles, and the survival of shell-forming marine organisms (Doney *et al.,* 2009). In this study, pH levels decreased as a result of increased oceanic DIC from the plastic-derived DIC flux. This was expected, as CO_2 is a component of DIC, and so an increase in DIC will ultimately increase H^+ concentrations. This decrease in pH (by 5.57×10^{-4} pH units) was very minor when compared to the decrease observed since preindustrial times (0.1 pH units or a 26% increase in H^+ concentrations; Caldeira & Wickett, 2005). The greatest decrease in globally averaged ocean surface pH was observed after the addition of the flux into the global coast; an increase in oceanic CO_2 in this region may be particularly harmful as this is where a large portion of calcifying organisms reside.

4.6 Ocean Alkalinity

As atmospheric CO_2 concentrations rise and CO_2 becomes dissolved in ocean waters, this results in a decrease in pH levels, leaving the normally basic ocean waters more acidic. The measure of alkalinity, or the buffering capacity, is the ability of a substance to resist change in pH. The excess of proton acceptors over donors is represented by total alkalinity (TA) and is denoted as: $TA = [HCO_3^-] + 2[CO_3^{2-}] + [OH^-] - [H^+]$ (Wolf-Gladrow *et al.,* 2007). Wolf-Gladrow *et al.,* (2007) further state that TA does not change as a result of the addition or depletion of CO_2 from or to the atmosphere. This is consistent with the results of this research which found that

oceanic alkalinity concentrations generally remained the same after the addition of the plastic-derived DIC flux. Although pH buffers, or proton acceptors, which include HCO_3^-, CO_3^{2-}, and OH^-, would bond with H+, the addition of DIC through the plastic-derived carbon flux would increase the concentrations of these buffers, resulting in negligible changes to ocean alkalinity. The greatest decrease in surface ocean alkalinity (by 2.60×10^{-5} mol m^{-3}) resulting from the addition of the plastic-derived DIC flux, was very minor when compared to the ocean's current mean ocean alkalinity (2.35 mol m^{-3}; Sarmiento & Gruber, 2006). This minor decrease can be attributed to the resultant increase in surface water acidity from increased CO_2 after the addition of the DIC flux. As more CO_2 is absorbed in surface waters, through the process of photosynthesis, these regions are more basic in comparison to deeper waters and so it was expected that alkalinity would be greater in surface waters.

4.7 Oceanic Oxygen Concentrations

As mentioned when discussing the solubility of CO_2 in water, increased air and ocean temperatures also reduce the solubility of oxygen. Solubility changes account for 15% of the total oxygen loss in ocean waters (50% in the upper 1000m) during 1960 – 2010 (Helm *et al.,* 2011; Schmidtko *et al.,* 2017). In addition, warmer waters are more buoyant than cooler waters; this increased stratification results in slower ocean circulation, preventing oxygen from mixing into deeper waters where it is needed for the breakdown of sinking organic matter. This reduced circulation is responsible for 50% of the observed deoxygenation in the upper 1000m of the ocean and 98% in deeper waters (Schmidtko *et al.,* 2017). Other, less impactful processes which may contribute to the deoxygenation of ocean waters include warming-induced respiration of organic matter and cessation of burial in sediments (Oschlies, 2019). In addition, nutrient inputs (ie. nitrogen and phosphorus) from agriculture and wastewater runoff result in an increase in phytoplankton which eventually dies off and decomposes, further depleting oxygen levels (Limburg *et al.,* 2020). 2% of oceanic oxygen content has been lost since the 1960s and an increase in oxygen minimum zones has been appearing in coastal waters and estuaries (Schmidtko *et al.,* 2017*)*. The consequences of these oxygen-depleted waters are a reduction in suitable habitats (habitat compression), a decrease in growth rate and reproduction, and an increase in disease susceptibility in organisms (Limburg *et al.,* 2020). In this study, the input of the plastic-derived DIC flux resulted in a very minor decrease in oxygen concentrations, by 9.46

x 10^{-6} mol m^{-3}; this occurred as temperatures increased due to the presence of additional CO_2 in the atmosphere.

4.8 Maximum Atlantic Meridional Overturning Circulation

The thermohaline circulation, also known as the meridional overturning, is characterized by the northward flow of warm, saline, shallow water, into the surface of the Atlantic Ocean, and the southward flow of cold, deeper water from the depths of the Labrador and Nordic Seas to the Southern Ocean. This global system of ocean currents brings nutrient-dense waters to the surface and regulates Earth's heat budget by counteracting the uneven distribution of solar radiation. As surface water temperatures are warming due to climate change, and increased precipitation and ice melt bring more freshwater into the ocean, the surface waters become more buoyant. Plastic-derived DIC had a very minor influence on the AMOC, as only relatively small fluctuations in the index were observed after the flux was added. The decrease in the AMOC index as a result of plastic-derived carbon leaching (-1.47 x 10^5 m^3 sec^{-1}) is minor when compared to the greatest decrease observed in the control integration, reaching 1.32 x 10^7 m^3 sec^{-1}.

The area of plastic-derived DIC flux input very minorly influenced the increase and decrease in atmospheric and oceanic tracers. The area of input resulting in the greatest change, most often, was the North Atlantic Ocean. These results were expected, as the Atlantic Ocean is the site of AMOC, where DIC in the surface ocean is transported to deeper waters. This is contrasting to ocean circulation in other ocean basins, such as the North Pacific Ocean and Indian Ocean, where DIC concentrations would more likely remain near the surface ocean for longer periods of time.

4.9 Land Soil Carbon

Soil organic matter is composed of bacteria and fungi, decaying materials including plant and animal tissues, and fecal matter. This matter contains high levels of carbon and is dependent on the interaction of ecosystem processes such as photosynthesis, respiration, and decomposition. Through these reactions, carbon is added or removed from the system and eventually reaches no net change in soil organic carbon levels (Ontl & Schulte, 2012). In the model, the addition of carbon to the land soil carbon stock is the result of plastic-derived carbon being outgassed as CO_2 to the atmosphere, where it is absorbed by the leaves of biota, and

deposited into the soil as litter. Eventually, this plastic-derived carbon is returned to the atmosphere through the respiration of soil carbon by soil biota. One-third of the total increase in atmospheric CO_2 concentrations results from soil organic carbon loss due to land use change (Lal, 2004). Carbon is released to the atmosphere through activities including deforestation and land use change (through the cultivation of land for agriculture), but soil carbon depletion is also occurring due to increased decomposition from warming soils after forest canopy removal (Ontl & Schulte, 2012). Depleted soil carbon sequestration is consequential for soil biodiversity and ultimately crop yield, however, it also presents an opportunity for the sequestration and storage of atmospheric CO_2 (Ontl & Schulte, 2012). The results of this study indicate that plastic-derived carbon leaching had a very minor effect on land soil carbon, with the greatest increase being 0.39 kg. This increase is evidently minor when comparing to values of land soil carbon stocks; 2500 Gt (2.50×10^{15} kg) of carbon is found in soil with 1550 Gt (1.55×10^{15} kg) being organic, and 950 Gt (9.50×10^{14} kg) being inorganic (Lal, 2004).

Chapter 5: Conclusions

Plastic pollution has become an ever-increasing environmental problem. Although serving many benefits across several industries, as a result of its mass production and poor waste management, plastic pollution is responsible for contributing to rising GHG emissions through its production and incineration, physical abrasions and reproductive health decline in marine organisms, the transport of invasive species, and the leaching of various compounds. Recent research has emerged that indicates that marine plastic pollution is leaching carbon into the marine environment and is potentially responsible for 10% of the DOC in the surface microlayer of heavily plastic-concentrated gyres (Romera-Castillo *et al*., 2018). Several researchers have indicated the need to quantify the amount of carbon being leached by plastics, relative to the total amount of carbon in the ocean and atmosphere (Adyel & Macreadie *et al*., 2022; Romera-Castillo *et al*., 2018). Moreover, researchers have stressed the importance of determining whether this leaching could be contributing to climate change.

The research presented in this thesis demonstrates the effect that global, large-scale plastic-derived carbon leaching may have on Earth's global climate system. With the use of the UVic ESCM, various modelling integrations were performed which involved adding carbon fluxes, based on current and projected marine plastic pollution values. This flux was added into the global ocean, global coast, and five subtropical gyres, for 100 or 500 years. The purpose of these modelling integrations was to determine whether upper-bound plastic-derived carbon leaching will result in significant changes in Earth's climate system through processes like oceanic and atmospheric warming, ocean acidification, and hypoxia, amongst others. Next, the effects on several oceanic and atmospheric variables (atmospheric CO_2 concentrations, SAT, oceanic DIC, ocean temperatures, ocean pH, ocean alkalinity, oceanic oxygen concentrations, AMOC, and land soil carbon) were analyzed.

Although recent research has emphasized the negative effects that plastic-derived carbon leaching in the marine environment may have on ecosystems and their biota, my results indicate that it has very minor and insignificant effects on Earth's global climate system.
When the results were compared to the control model integration which only included emissions from anthropogenic fossil fuel combustion based on RCP 8.5, changes in the measured oceanic and atmospheric tracers as a result of plastic-derived carbon leaching were <1%. Although plastic pollution threatens the livelihood of many organisms and the ecosystems in which they

reside, the results of my study conclude that emissions from plastic-derived carbon leaching should not be of concern in relation to climate change. Where the greater focus is needed, is on the prevention of plastic incineration and production emissions, but most importantly, those from fossil fuel combustion.

References

Addamo AM, Laroche P, Hanke G. 2017. Top marine beach litter items in Europe. A review and synthesis based on beach litter data. MSFD Technical group on marine litter. Report No. EUR29249. doi:10.2760/496717, JRC108181

Adyel TM. 2020. Accumulation of plastic waste during COVID-19. Science, 369(6509), 1314-1315. https://doi.org/10.1126/science.abd9925.

Adyel TM, Macreadie PI. 2022. Plastics in blue carbon ecosystems: a call for global cooperation on climate change goals. The Lancet Planetary Health, 6(1), e2-e3. https://doi.org/10.1016/S2542-5196(21)00327-2.

Ahmad M, Bajahlan AS. 2007. Leaching of styrene and other aromatic compounds in drinking water from PS bottles. Journal of Environmental Sciences, 19(4), 421-426. https://doi.org/10.1016/S1001-0742(07)60070-9.

Anderson KA, Hillwalker WE. 2008. Encyclopedia of Ecology.

Andrady AL. 2011. Microplastics in the marine environment. Marine Pollution Bulletin, 62(8), 1596-1605. https://doi.org/10.1016/j.marpolbul.2011.05.030.

Andrady AL, Neal MA. 2009. Applications and societal benefits of plastics. Philosophical Transactions of the Royal Society B: Biological Sciences, 364(1526), 1977-1984. https://doi.org/10.1098/rstb.2008.0304.

Archer DE. 1996. An atlas of the distribution of calcium carbonate in sediments of the deep sea. Global Biogeochemical Cycles, 10(1), 159-174. https://doi.org/10.1029/95GB03016.

Avio CG, Gorbi S, Regoli F. 2017. Plastics and microplastics in the oceans: from emerging pollutants to emerged threat. Marine environmental research, 128, 2-11. https://doi.org/10.1016/j.marenvres.2016.05.012.

Baekeland LH. 1909. The synthesis, constitution, and uses of Bakelite. Industrial & Engineering Chemistry, 1(3), 149-161.

Barnes DK, Galgani F, Thompson RC, Barlaz M. 2009. Accumulation and fragmentation of plastic debris in global environments. Philosophical transactions of the royal society B: biological sciences, 364(1526), 1985-1998. https://doi.org/10.1098/rstb.2008.0205.

Biagi E, Musella M, Palladino G, Angelini V, Pari S, Roncari C, Candela, M, et al. 2021. Impact of plastic debris on the gut microbiota of Caretta caretta from Northwestern Adriatic Sea. Frontiers in Marine Science, 8, 637030. https://doi.org/10.3389/fmars.2021.637030.

Bitz CM, Holland MM, Weaver AJ, Eby M. 2001. Simulating the ice-thickness distribution in a coupled climate model. Journal of Geophysical Research: Oceans, 106(C2), 2441-2463. https://doi.org/10.1029/1999JC000113.

Boerger CM, Lattin GL, Moore SL, Moore CJ. 2010. Plastic ingestion by planktivorous fishes in the North Pacific Central Gyre. Marine Pollution Bulletin, 60(12), 2275-2278. https://doi.org/10.1016/j.marpolbul.2010.08.007.

Botterell ZL, Beaumont N, Cole M, Hopkins FE, Steinke M, Thompson RC, Lindeque PK. 2020. Bioavailability of microplastics to marine zooplankton: effect of shape and infochemicals. Environmental Science & Technology, 54(19), 12024-12033. https://doi.org/10.1021/acs.est.0c02715.

Caldeira K, Wickett ME. 2005. Ocean model predictions of chemistry changes from carbon dioxide emissions to the atmosphere and ocean. Journal of Geophysical Research: Oceans, 110(C9). https://doi.org/10.1029/2004JC002671.

Carpenter EJ, Anderson SJ, Harvey GR, Miklas HP, Peck BB. 1972. Polystyrene spherules in coastal waters. Science, 178(4062), 749-750. https://doi.org/10.1126/science.175.4027.1240.

Carpenter EJ, Smith Jr KL. 1972. Plastics on the Sargasso Sea surface. Science, 175(4027), 1240-1241. https://doi.org/10.1126/science.175.4027.1240.

Caruso G, Bergami E, Singh N, Corsi I. 2022. Plastic occurrence, sources, and impacts in Antarctic environment and biota. Water Biology and Security, 100034. https://doi.org/10.1016/j.watbs.2022.100034.

Chassignet EP, Xu X, Zavala-Romero O. 2021. Tracking marine litter with a global ocean model: where does it go? Where does it come from? Frontiers in Marine Science, 8, 667591. https://doi.org/10.3389/fmars.2021.667591.

Cheng J, Jacquin J, Conan P, Pujo-Pay M, Barbe V, George M, Ghiglione JF. 2021. Relative influence of plastic debris size and shape, chemical composition and phytoplankton-bacteria interactions in driving seawater plastisphere abundance, diversity and activity. Frontiers in Microbiology, 11, 610231. https://doi.org/10.3389/fmicb.2020.610231.

Cole M, Lindeque P, Fileman E, Halsband C, Goodhead R, Moger J, Galloway TS. 2013. Microplastic ingestion by zooplankton. Environmental Science & Technology, 47(12), 6646-6655. https://doi.org/10.1021/es400663f.

Colton Jr JB, Burns BR, Knapp FD. 1974. Plastic Particles in Surface Waters of the Northwestern Atlantic: The abundance, distribution, source, and significance of various types of plastics are discussed. Science, 185(4150), 491-497. https://doi.org/10.1126/science.185.4150.491.

Cox PM. 2001. Description of the" TRIFFID" dynamic global vegetation model.

Cózar A, Echevarría F, González-Gordillo JI, Irigoien X, Úbeda B, Hernández-León S, Duarte CM, et al. 2014. Plastic debris in the open ocean. Proceedings of the National Academy of Sciences, 111(28), 10239-10244. https://doi.org/10.1073/pnas.1314705111.

Dai A, Luo D, Song M, Liu J. 2019. Arctic amplification is caused by sea-ice loss under increasing CO2. Nature Communications, 10(1), 121. https://doi.org/10.1038/s43247-022-00498-3.

Dawson AL, Kawaguchi S, King CK, Townsend KA, King R, Huston WM, Bengtson Nash SM. 2018. Turning microplastics into nanoplastics through digestive fragmentation by Antarctic krill. Nature Communications, 9(1), 1001. https://doi.org/10.1038/s41467-018-03465-9.

Dobler D, Huck T, Maes C, Grima N, Blanke B, Martinez E, Ardhuin F. 2019. Large impact of Stokes drift on the fate of surface floating debris in the South Indian Basin. Marine Pollution Bulletin, 148, 202-209. https://doi.org/10.1016/j.marpolbul.2019.07.057.

Doney SC, Fabry VJ, Feely RA, Kleypas JA. 2009. Ocean acidification: the other CO_2 problem. Annual Review of Marine Science, 1, 169-192. https://doi.org/10.1146/annurev.marine.010908.163834.

Dussud C, Ghiglione JF. 2014. Bacterial degradation of synthetic plastics. In CIESM Workshop Monographs, 46, 49-54.

Ebbesmeyer C, Scigliano E. 2010. Flotsametrics and the floating world. Harper Collins, New York.

Eby M, Zickfeld K, Montenegro A, Archer D, Meissner KJ, Weaver AJ. 2009. Lifetime of anthropogenic climate change: millennial time scales of potential CO2 and surface temperature perturbations. Journal of Climate, *22*(10), 2501-2511. https://doi.org/10.1175/2008JCLI2554.1.

Eriksen M, Lebreton LC, Carson HS, Thiel M, Moore CJ, Borerro JC, Reisser J, et al. 2014. Plastic pollution in the world's oceans: more than 5 trillion plastic pieces weighing over 250,000 tons afloat at sea. PloS one, 9(12), e111913. https://doi.org/10.1371/journal.pone.0111913.

Eriksen M, Thiel M, Lebreton L. 2019. Nature of plastic marine pollution in the subtropical gyres. Hazardous Chemicals Associated with Plastics in the Marine Environment, 135-162. https://doi.org/10.1007/698_2016_123.

Eunomia. 2016. “Plastics in the Marine Environment.” https://safety4sea.com/wp-content/uploads/2016/06/Eunomia-Plastics-in-the-MarineEnvironment-2016_06.pdf.

Evans CD, Monteith DT, Cooper DM. 2005. Long-term increases in surface water dissolved organic carbon: observations, possible causes and environmental impacts. Environmental Pollution, 137(1), 55-71. https://doi.org/10.1016/j.envpol.2004.12.031.

Fanning AF, Weaver AJ. 1996. An atmospheric energy-moisture balance model: Climatology, interpentadal climate change, and coupling to an ocean general circulation model. Journal of Geophysical Research: Atmospheres, 101(D10), 15111-15128. https://doi.org/10.1029/96JD01017.

Feely RA, Sabine CL, Takahashi T, Wanninkhof R. 2001. Uptake and storage of carbon dioxide in the ocean: The global co~ 2 survey. Oceanography-Washington DC-Oceanography Society, 14(4), 18-32.

Fischer V, Elsner NO, Brenke N, Schwabe E, Brandt A. 2015. Plastic pollution of the Kuril–Kamchatka Trench area (NW pacific). Deep Sea Research Part II: Topical Studies in Oceanography, 111, 399-405. https://doi.org/10.1016/j.dsr2.2014.08.012.

Frias JP, Nash R. 2019. Microplastics: Finding a consensus on the definition. Marine Pollution Bulletin, 138, 145-147. https://doi.org/10.1016/j.marpolbul.2018.11.022.

Friedlingstein P, Jones MW, O'Sullivan M, Andrew RM, Bakker DC, Hauck J, Zeng J. 2022. Global carbon budget 2021. Earth System Science Data, 14(4), 1917-2005. https://doi.org/10.5194/essd-14-1917-2022.

García-Gómez JC, Garrigós M, Garrigós J. 2021. Plastic as a vector of dispersion for marine species with invasive potential. A review. Frontiers in Ecology and Evolution, 9, 629756. https://doi.org/10.3389/fevo.2021.629756.

GESAMP. 2016. “Sources, Fate and Effects of Microplastics in the Marine Environment: Part Two of a Global Assessment” 93: 17–18.

Gewert B, Plassmann MM, MacLeod M. 2015. Pathways for degradation of plastic polymers floating in the marine environment. Environmental Science: Processes & Impacts, 17(9), 1513-1521. https://doi.org/10.1039/C5EM00207A.

Geyer R, Jambeck JR, Law KL. 2017. Production, use, and fate of all plastics ever made. Science Advances, 3(7), e1700782. https://doi.org/10.1126/sciadv.1700782.

Grant ML, Lavers JL, Hutton I, Bond AL. 2021. Seabird breeding islands as sinks for marine plastic debris. Environmental Pollution, 276, 116734. https://doi.org/10.1016/j.envpol.2021.116734.

Grebmeier JM, Barry JP. 2007. Benthic processes in polynyas. Elsevier Oceanography Series, 74, 363-390. https://doi.org/10.1016/S0422-9894(06)74011-9.

Guo X, Wang J. 2019. Sorption of antibiotics onto aged microplastics in freshwater and seawater. Marine Pollution Bulletin, 149, 110511. https://doi.org/10.1016/j.marpolbul.2019.110511.

Haigh R, Ianson D, Holt CA, Neate HE, Edwards AM. 2015. Effects of ocean acidification on temperate coastal marine ecosystems and fisheries in the Northeast Pacific. PLoS One, 10(2), e0117533. https://doi.org/10.1371/journal.pone.0117533.

Hakkarainen M, Albertsson AC. 2004. Environmental degradation of polyethylene. Long Term Properties of Polyolefins, 177-200. https://doi.org/10.1007/b13523.

Hansell DA. 2013. Recalcitrant dissolved organic carbon fractions. Annual Review of Marine Science, 5, 421-445. https://doi.org/10.1146/annurev-marine-120710-100757.

Hansell DA, Carlson CA, Repeta DJ, Schlitzer R. 2009. Dissolved organic matter in the ocean: A controversy stimulates new insights. Oceanography, *22*(4), 202-211. https://www.jstor.org/stable/24861036.

Helm KP, Bindoff NL, Church JA. 2011. Observed decreases in oxygen content of the global ocean. Geophysical Research Letters, 38(23). https://doi.org/10.1029/2011GL049513.

Hunke EC, Dukowicz JK. 1997. An elastic–viscous–plastic model for sea ice dynamics. Journal of Physical Oceanography, 27(9), 1849-1867. https://doi.org/10.1175/1520-0485(1997)027%3C1849:AEVPMF%3E2.0.CO;2.

IPCC. 2008. Towards new scenarios for analysis of emissions, climate change, impacts, and response strategies. IPCC Expert Meeting Report on New Scenarios, Noordwijkerhout, Intergovernmental Panel on Climate Change.

IPCC. 2021. Climate Change 2021: The Physical Science Basis. Contribution of Working Group I to the Sixth Assessment Report of the Intergovernmental Panel on Climate Change [Masson-Delmotte, V., P. Zhai, A. Pirani, S.L. Connors, C. Péan, S. Berger, N. Caud, Y. Chen, L. Goldfarb, M.I. Gomis, M. Huang, K. Leitzell, E. Lonnoy, J.B.R. Matthews, T.K. Maycock, T. Waterfield, O. Yelekçi, R. Yu, and B. Zhou (eds.)]. In Press.

Isobe A, Iwasaki S. 2022. The fate of missing ocean plastics: Are they just a marine environmental problem? Science of the Total Environment, 825, 153935. https://doi.org/10.1016/j.scitotenv.2022.153935.

Isobe A, Kubo K, Tamura Y, Nakashima E, Fujii N. 2014. Selective transport of microplastics and mesoplastics by drifting in coastal waters. Marine Pollution Bulletin, 89(1-2), 324-330. https://doi.org/10.1016/j.marpolbul.2014.09.041.

Iwasaki S, Isobe A, Kako SI, Uchida K, Tokai T. 2017. Fate of microplastics and mesoplastics carried by surface currents and wind waves: A numerical model approach in the Sea of Japan. Marine Pollution Bulletin, 121(1-2), 85-96. https://doi.org/10.1016/j.marpolbul.2017.05.057.

Jambeck JR, Geyer R, Wilcox C, Siegler TR, Perryman M, Andrady A, Law K. L. 2015. Plastic waste inputs from land into the ocean. Science, 347(6223), 768-771. https://doi.org/10.1126/science.1260352.

Jamieson AJ, Brooks LSR, Reid WD, Piertney SB, Narayanaswamy BE, Linley TD. 2019. Microplastics and synthetic particles ingested by deep-sea amphipods in six of the deepest marine ecosystems on Earth. Royal Society Open Science, 6(2), 180667. https://doi.org/10.1098/rsos.180667.

Jones-Williams K, Galloway TS, Peck VL, Manno C. 2021. Remote, but Not Isolated—Microplastics in the Sub-surface Waters of the Canadian Arctic Archipelago. Frontiers in Marine Science, 8, 666482. https://doi.org/10.3389/fmars.2021.666482.

Kalnay E, Kanamitsu M, Kistler R, Collins W, Deaven D, Gandin L, Joseph D, et al. 1996. The NCEP/NCAR 40-year reanalysis project. Bulletin of the American Meteorological Society, 77(3), 437-472. https://doi.org/10.1175/1520-0477(1996)077%3C0437:TNYRP%3E2.0.CO;2.

Kane IA, Clare MA, Miramontes E, Wogelius R, Rothwell JJ, Garreau P, Pohl F. 2020. Seafloor microplastic hotspots controlled by deep-sea circulation. Science, 368(6495), 1140-1145. https://doi.org/10.1126/science.aba5899.

Kenyon KW, Kridler E. 1969. Laysan albatrosses swallow indigestible matter. The Auk, 86(2), 339-343. https://doi.org/10.2307/4083505.

Kowalski N, Reichardt AM, Waniek JJ. 2016. Sinking rates of microplastics and potential implications of their alteration by physical, biological, and chemical factors. Marine Pollution Bulletin, 109(1), 310-319. https://doi.org/10.1016/j.marpolbul.2016.05.064.

Kukulka T, Proskurowski G, Morét-Ferguson S, Meyer DW, Law KL. 2012. The effect of wind mixing on the vertical distribution of buoyant plastic debris. Geophysical Research Letters, 39(7). https://doi.org/10.1029/2012GL051116.

Lal R. 2004. Soil carbon sequestration impacts on global climate change and food security. Science, 304(5677), 1623-1627. https://doi.org/10.1126/science.1097396.

Lambert S, Wagner M. 2016. Characterisation of nanoplastics during the degradation of polystyrene. Chemosphere, 145, 265-268. https://doi.org/10.1016/j.chemosphere.2015.11.078.

Lau WW, Shiran Y, Bailey RM, Cook E, Stuchtey MR, Koskella J, Palardy J, et al. 2020. Evaluating scenarios toward zero plastic pollution. Science, 369(6510), 1455 1461. https://doi.org/10.1126/science.aba9475.

Law KL, Morét-Ferguson SE, Goodwin DS, Zettler ER, DeForce E, Kukulka T, Proskurowski G. 2014. Distribution of surface plastic debris in the eastern Pacific Ocean from an 11-year data set. Environmental Science & Technology, 48(9), 4732-4738. https://doi.org/10.1021/es4053076.

Law KL, Morét-Ferguson S, Maximenko NA, Proskurowski G, Peacock EE, Hafner J, Reddy CM. 2010. Plastic accumulation in the North Atlantic subtropical gyre. Science, 329(5996), 1185-1188. https://doi.org/10.1126/science.1192321.

Law KL, Starr N, Siegler TR, Jambeck JR, Mallos NJ, Leonard GH. 2020. The United States' contribution of plastic waste to land and ocean. Science Advances, 6(44), eabd0288. https://doi.org/10.1126/sciadv.abd0288.

Lebreton L, Andrady A. 2019. Future scenarios of global plastic waste generation and disposal. Palgrave Communications, 5(1), 1-11. https://doi.org/10.1057/s41599-018-0212-7.

Lebreton L, Egger M, Slat B. 2019. A global mass budget for positively buoyant macroplastic debris in the ocean. Scientific Reports, 9(1), 12922. https://doi.org/10.1038/s41598-019-49413-5.

Lebreton L, Royer SJ, Peytavin A, Strietman WJ, Smeding-Zuurendonk I, Egger M. 2022. Industrialised fishing nations largely contribute to floating plastic pollution in the North Pacific subtropical gyre. Scientific Reports, 12(1), 12666. https://doi.org/10.1038/s41598-022-16529-0.

Lebreton L, Slat B, Ferrari F, Sainte-Rose B, Aitken J, Marthouse R, Reisser J, et al. 2018. Evidence that the Great Pacific Garbage Patch is rapidly accumulating plastic. Scientific Reports, 8(1), 1-15. https://doi.org/10.1038/s41598-018-22939-w.

Lebreton LC, Van Der Zwet J, Damsteeg JW, Slat B, Andrady A, Reisser J. 2017. River plastic emissions to the world's oceans. Nature Communications, 8(1), 15611. https://doi.org/10.1038/ncomms15611.

Lerman A. 2009. Carbon cycle. In Encyclopedia of Earth Sciences Series, 983-986. Springer Netherlands. https://doi.org/10.1007/978-1-4020-4411-3_28.

Leslie HA, Van Velzen MJ, Brandsma SH, Vethaak AD, Garcia-Vallejo JJ, Lamoree MH. 2022. Discovery and quantification of plastic particle pollution in human blood. Environment International, 163, 107199. https://doi.org/10.1016/j.envint.2022.107199.

Likens GE. 2009. Encyclopedia of Inland Waters. Elsevier.

Limburg KE, Breitburg D, Swaney DP, Jacinto G. 2020. Ocean deoxygenation: A primer. One Earth, 2(1), 24-29. https://doi.org/10.1016/j.oneear.2020.01.001.

Liu Y, Moore JK, Primeau F, Wang WL. 2022. Reduced CO_2 uptake and growing nutrient sequestration from slowing overturning circulation. Nature Climate Change, 1-8. https://doi.org/10.1038/s41558-022-01555-7.

Liubartseva S, Coppini G, Lecci R, Creti S. 2016. Regional approach to modeling the transport of floating plastic debris in the Adriatic Sea. Marine Pollution Bulletin, 103(12), 115-127. https://doi.org/10.1016/j.marpolbul.2015.12.031.

Lønborg C, Carreira C, Jickells T, Álvarez-Salgado XA. 2020. Impacts of global change on ocean dissolved organic carbon (DOC) cycling. Frontiers in Marine Science, 7, 466. https://doi.org/10.3389/fmars.2020.00466.

Loughlin C, Mendes ARM, Morrison L, Morley A. 2021. The role of oceanographic processes and sedimentological settings on the deposition of microplastics in marine sediment: Icelandic waters. Marine Pollution Bulletin, 164, 111976. https://doi.org/10.1016/j.marpolbul.2021.111976.

Lu JX, Tupper C, Murray J. 2017. Biochemistry, dissolution and solubility. StatPearls. https://www.ncbi.nlm.nih.gov/books/NBK431100/.

Mafuta C, Baker E, Rucevska I, Thygesen K, Appelquist LR, Westerveld L, Schoolmeester T, et al. 2021. Drowning in Plastics: Marine Litter and Plastic Waste Vital Graphics.https://wedocs.unep.org/xmlui/bitstream/handle/20.500.11822/36964/VITGRAPH.pdf.

Martinez E, Maamaatuaiahutapu K, Taillandier V. 2009. Floating marine debris surface drift: convergence and accumulation toward the South Pacific subtropical gyre. Marine Pollution Bulletin, 58(9), 1347-1355. https://doi.org/10.1016/j.marpolbul.2009.04.022.

McKinsey Center for Business and Environment. 2015 Stemming the tide: land-based strategies for a plastic-free ocean. McKinsey & Company and Ocean Conservancy.

Meijer LJ, Van Emmerik T, Van Der Ent R, Schmidt C, Lebreton L. 2021. More than 1000 rivers account for 80% of global riverine plastic emissions into the ocean. Science Advances, 7(18), eaaz5803. https://doi.org/10.1126/sciadv.aaz5803.

Meissner KJ, Weaver AJ, Matthews HD, Cox PM. 2003. The role of land surface dynamics in glacial inception: a study with the UVic Earth System Model. Climate Dynamics, 21, 515-537. https://doi.org/10.1007/s00382-003-0352-2.

Montoto-Martínez T, De la Fuente J, Puig-Lozano R, Marques N, Arbelo M, Hernández Brito JJ, Gelado-Caballero MD, et al. 2021. Microplastics, bisphenols, phthalates and pesticides in odontocete species in the Macaronesian Region (Eastern North Atlantic). Marine Pollution Bulletin, 173, 113105. https://doi.org/10.1016/j.marpolbul.2021.113105.

Morales-Caselles C, Viejo J, Martí E, González-Fernández D, Pragnell-Raasch H, González-Gordillo JI, Cózar A, et al. 2021. An inshore–offshore sorting system revealed from global classification of ocean litter. Nature Sustainability, 4(6), 484-493. https://doi.org/10.1038/s41893-021-00720-8.

Morét-Ferguson S, Law KL, Proskurowski G, Murphy EK, Peacock EE, Reddy CM. (2010). The size, mass, and composition of plastic debris in the western North Atlantic Ocean. Marine Pollution Bulletin, 60(10), 1873-1878. https://doi.org/10.1016/j.marpolbul.2010.07.020.

Morris RJ. 1980. Plastic debris in the surface waters of the South Atlantic. Marine Pollution Bulletin, 11(6), 164-166. https://doi.org/10.1016/0025-326X(80)90144-7.

Naji A, Nuri M, Vethaak AD. 2018. Microplastics contamination in molluscs from the northern part of the Persian Gulf. Environmental Pollution, 235, 113-120. https://doi.org/10.1016/j.envpol.2017.12.046.

NOAA. National Oceanic and Atmospheric Administration. 2019. Carbon cycle. https://www.noaa.gov/education/resource-collections/climate/carbon-cycle.

Obbard RW. 2018. Microplastics in polar regions: the role of long range transport. Current Opinion in Environmental Science & Health, 1, 24-29. https://doi.org/10.1016/j.coesh.2017.10.004.

Obbard RW, Sadri S, Wong YQ, Khitun AA, Baker I, Thompson RC. 2014. Global warming releases microplastic legacy frozen in Arctic Sea ice. Earth's Future, 2(6), 315-320. https://doi.org/10.1002/2014EF000240.

Ontl TA, Schulte LA. 2012. Soil carbon storage. Nature Education Knowledge, 3(10). https://www.pacificwolves.org/wp-content/uploads/2019/06/Ontl-and-Schulte_2012.pdf.

Orr JC. 1999. On ocean carbon-cycle model comparison. Tellus B: Chemical and Physical Meteorology, 51(2), 509-510. https://doi.org/10.3402/tellusb.v51i2.16334.

Orr JC, Fabry VJ, Aumont O, Bopp L, Doney SC, Feely RA, Yool A, et al. 2005. Anthropogenic ocean acidification over the twenty-first century and its impact on calcifying organisms. Nature, 437(7059), 681-686. https://doi.org/10.1038/nature04095.

Oschlies A. 2019. Ocean deoxygenation from climate change. IUCN. https://portals.iucn.org/library/sites/library/files/documents/03.1%20DEOX.pdf.

Pacanowski RC. 1995. MOM 2 documentation, user's guide and reference manual. Tech Rep 3, GFDL Ocean Group, Geophysical Fluid Dynamics Laboratory, Princeton, USA

Pace NR. 2001. The universal nature of biochemistry. Proceedings of the National Academy of Sciences, 98(3), 805-808. https://doi.org/10.1073/pnas.98.3.805.

Paluselli A, Fauvelle V, Galgani F, Sempere R. 2018. Phthalate release from plastic fragments and degradation in seawater. Environmental Science & Technology, 53(1), 166 175. https://doi.org/10.1021/acs.est.8b05083.

Plastics Europe. 2021. "Plastics - the Facts 2021." https://plasticseurope.org/wpcontent/uploads/2021/12/Plastics-the-Facts-2021-webfinal.pdf

PlasticsEurope, EUPC, EPRO, E. 2006. The compelling facts about plastics. An Analysis of Plastics Production, Demand and Recovery for 2006 in Europe. https://plasticseurope.org/wp-content/uploads/2021/10/2006-Compelling-facts.pdf.

Prinz N, Korez Š. 2020. Understanding how microplastics affect marine biota on the cellular level is important for assessing ecosystem function: a review. In YOUMARES 9 The Oceans: Our Research, Our Future: Proceedings of the 2018 conference for YOUng MArine RESearcher in Oldenburg, Germany, 101-120. Springer International Publishing. https://doi.org/10.1007/978-3-030-20389-4.

Rantanen M, Karpechko AY, Lipponen A, Nordling K, Hyvärinen O, Ruosteenoja K, Laaksonen, A, et al. 2022. The Arctic has warmed nearly four times faster than the globe since 1979. Communications Earth & Environment, 3(1), 168. https://doi.org/10.1038/s43247-022-00498-3.

Reddy MS, Basha S, Adimurthy S, Ramachandraiah G. 2006. Description of the small plastics fragments in marine sediments along the Alang-Sosiya ship-breaking yard, India. Estuarine, Coastal and Shelf Science, 68(3-4), 656-660. https://doi.org/10.1016/j.ecss.2006.03.018.

Reisser J, Slat B, Noble K, Du Plessis K, Epp M, Proietti M, Pattiaratchi C, et al. 2015. The vertical distribution of buoyant plastics at sea: an observational study in the North Atlantic Gyre. Biogeosciences, 12(4), 1249-1256. https://doi.org/10.5194/bg-12-1249-2015.

Romera-Castillo C, Pinto M, Langer TM, Álvarez-Salgado XA, Herndl GJ. 2018. Dissolved organic carbon leaching from plastics stimulates microbial activity in the ocean. Nature Communications, 9(1), 1430. https://doi.org/10.1038/s41467-018-03798-5.

Rothstein SI. 1973. Plastic particle pollution of the surface of the Atlantic Ocean: evidence from a seabird. The Condor, 75(3), 344-345. https://doi.org/10.2307/1366176.

Sarmiento JL, Gruber N. 2006. Ocean Biogeochemical Dynamics. Princeton University Press. https://doi.org/10.2307/j.ctt3fgxqx.

Schmidt C, Krauth T, Wagner S. 2017. Export of plastic debris by rivers into the sea. Environmental Science & Technology, 51(21), 12246-12253. https://doi.org/10.1021/acs.est.7b02368.

Schmidtko S, Stramma L, Visbeck M. 2017. Decline in global oceanic oxygen content during the past five decades. Nature, 542(7641), 335-339. https://doi.org/10.1038/nature21399.

Schmittner, A., Oschlies, A., Matthews, H. D., & Galbraith, E. D. (2008). Future changes in climate, ocean circulation, ecosystems, and biogeochemical cycling simulated for a business-as-usual CO_2 emission scenario until year 4000 AD. *Global Biogeochemical Cycles*, *22*(1). https://doi.org/10.1029/2007GB002953.

Setälä O, Fleming-Lehtinen V, Lehtiniemi M. 2014. Ingestion and transfer of microplastics in the planktonic food web. Environmental Pollution, 185, 77-83. https://doi.org/10.1016/j.envpol.2013.10.013.

Shaw DG. 1977. Pelagic tar and plastic in the Gulf of Alaska and Bering Sea: 1975. Science of the Total Environment, 8(1), 13-20. https://doi.org/10.1016/0048-9697(77)90058-4.

Takahashi T, Feely RA, Weiss RF, Wanninkhof RH, Chipman DW, Sutherland SC, Takahashi TT. 1997. Global air-sea flux of CO_2: An estimate based on measurements of sea–air pCO_2 difference. Proceedings of the National Academy of Sciences, 94(16), 8292-8299. https://doi.org/10.1073/pnas.94.16.8292.

Taylor ML, Gwinnett C, Robinson LF, Woodall LC. 2016. Plastic microfiber ingestion by deep-sea organisms. Scientific Reports, 6(1), 33997. https://doi.org/10.1038/srep33997.

Teuten EL, Saquing JM, Knappe DR, Barlaz MA, Jonsson S, Björn A, Takada H. 2009. Transport and release of chemicals from plastics to the environment and to wildlife. Philosophical Transactions of the Royal Society B: Biological Sciences, 364(1526), 2027-2045. https://doi.org/10.1098/rstb.2008.0284.

Thompson RC, Swan SH, Moore CJ, Vom Saal FS. 2009. Our plastic age. Philosophical Transactions of the Royal Society B: Biological Sciences, 364(1526), 1973-1976. https://doi.org/10.1098/rstb.2009.0054.

Thushari GGN, Senevirathna JDM. 2020. Plastic pollution in the marine environment. Heliyon, 6(8), e04709. https://doi.org/10.1016/j.heliyon.2020.e04709.

Trusts PC. 2020. SYSTEMIQ. "Breaking the plastic wave: A comprehensive assessment of pathways towards stopping ocean plastic pollution."

Turra A, Manzano AB, Dias RJS, Mahiques MM, Barbosa L, Balthazar-Silva D, Moreira, FT. 2014. Three-dimensional distribution of plastic pellets in sandy beaches: shifting paradigms. Scientific Reports, 4(1), 4435. https://doi.org/10.1038/srep04435.

United Nations Environment Programme. 2021. From Pollution to Solution: A global assessment of marine litter and plastic pollution. Nairobi.

Van Cauwenberghe L, Vanreusel A, Mees J, Janssen CR. 2013. Microplastic pollution in deep-sea sediments. Environmental Pollution, 182, 495-499. https://doi.org/10.1016/j.envpol.2013.08.013.

Venrick EL, Backman TW, Bartram WC, Platt CJ, Thornhill MS, Yates RE. 1973. Man-made objects on the surface of the central North Pacific Ocean. Nature, 241(5387), 271-271. https://doi.org/10.1038/241271a0

Verla AW, Enyoh CE, Verla EN, Nwarnorh KO. 2019. Microplastic–toxic chemical interaction: a review study on quantified levels, mechanism and implication. SN Applied Sciences, 1(11), 1-30. https://doi.org/10.1007/s42452-019-1352-0.

Wang Q, Bai J, Ning B, Fan L, Sun T, Fang Y, Gao Z. 2020. Effects of bisphenol A and nanoscale and microscale polystyrene plastic exposure on particle uptake and toxicity in human Caco-2 cells. Chemosphere, 254, 126788. https://doi.org/10.1016/j.chemosphere.2020.126788.

Weaver AJ, Eby M, Wiebe EC, Bitz CM, Duffy PB, Ewen TL, Yoshimori M, et al. 2001. The UVic Earth System Climate Model: Model description, climatology, and applications to past, present and future climates. Atmosphere-Ocean, 39(4), 361-428. https://doi.org/10.1080/07055900.2001.9649686.

Weijer W, Veneziani M, Stössel A, Hecht MW, Jeffery N, Jonko A, Wang H, et al. 2017. Local atmospheric response to an open-ocean polynya in a high-resolution climate model. Journal of Climate, 30(5), 1629-1641. https://doi.org/10.1175/JCLI-D-16-0120.1.

Willey JD, Kieber RJ, Eyman MS, Avery Jr GB. 2000. Rainwater dissolved organic carbon: concentrations and global flux. Global Biogeochemical Cycles, 14(1), 139-148. https://doi.org/10.1029/1999GB900036.

Wolf-Gladrow DA, Zeebe RE, Klaas C, Körtzinger A, Dickson AG. 2007. Total alkalinity: The explicit conservative expression and its application to biogeochemical processes. Marine Chemistry, 106(1-2), 287-300. https://doi.org/10.1016/j.marchem.2007.01.006.

Wong CS, Green DR, Cretney WJ. 1974. Quantitative tar and plastic waste distributions in the Pacific Ocean. Nature, 247, 30-32. https://doi.org/10.1038/247030a0.

Wright SL, Thompson RC, Galloway TS. 2013. The physical impacts of microplastics on marine organisms: a review. Environmental Pollution, 178, 483-492. https://doi.org/10.1016/j.envpol.2013.02.031.

Yamashita R, Tanimura A. 2007. Floating plastic in the Kuroshio current area, western North Pacific Ocean. Marine Pollution Bulletin, 4(54), 485-488. http://dx.doi.org/10.1016%2Fj.marpolbul.2006.11.012.

Yan J, Lin Q, Poh SC, Li Y, Zhan L. 2020. Underway measurement of dissolved inorganic carbon (DIC) in estuarine waters. Journal of Marine Science and Engineering, 8(10), 765. https://doi.org/10.3390/jmse8100765.

Yarsley VE, Couzens EG. 1945. Plastics. Middlesex: Penguin Books Limited.

Yu X, Ladewig S, Bao S, Toline CA, Whitmire S, Chow AT. 2018. Occurrence and distribution of microplastics at selected coastal sites along the southeastern United States. Science of the Total Environment, 613, 298-305. https://doi.org/10.1016/j.scitotenv.2017.09.100.

Zettler ER, Mincer TJ, Amaral-Zettler LA. 2013. Life in the "plastisphere": microbial communities on plastic marine debris. Environmental Science & Technology, 47(13), 7137-7146. https://doi.org/10.1021/es401288x.

Zhu L, Zhao S, Bittar TB, Stubbins A, Li D. 2020. Photochemical dissolution of buoyant microplastics to dissolved organic carbon: rates and microbial impacts. Journal of Hazardous Materials, 383, 121065. https://doi.org/10.1016/j.jhazmat.2019.121065.

Zhu X. 2021. The plastic cycle–an unknown branch of the carbon cycle. Frontiers in Marine Science, 1227. https://doi.org/10.3389/fmars.2020.609243.